Disease severity in coinfected hosts: the importance of infection order

Aloïs Dusuel[1*], Luc Bourbon[2*], Emma Groetz[1], Nicolas Pernet[3], Mickaël Rialland[1], Benjamin Roche[4,5], Bruno Faivre[2], Gabriele Sorci[2#]

1. CTM - Center for Translational and Molecular Medicine, INSERM UMR 1231, Université de Bourgogne, 21000 Dijon, France ; LabEx LipSTIC, 21000 Dijon, France

2. Biogéosciences, CNRS UMR 6282, Université de Bourgogne, 6 Boulevard Gabriel, 21000 Dijon, France

3. Plateforme ImaFlow, Université de Bourgogne, Inserm, Institut Agro Dijon, CGFL, CHU Dijon Bourgogne, US58 BioSanD, F-21000 Dijon, France

4. MIVEGEC, IRD, CNRS, Université de Montpellier, 34090 Montpellier, France

5. International Joint Laboratory ELDORADO, IRD/UNAM, Mérida, Yucatán, México

#corresponding author: gabriele.sorci@u-bourgogne.fr

*equal contribution

Abstract

When hosts are simultaneously infected by different pathogens, the severity of the disease might be altered compared to hosts harboring single infections. The reasons underlying these changes in parasite virulence are manifold. Here, we investigated the importance of order and timing of infection. We used a model of rodent coinfection between two parasites that do not compete for common resources, an intestinal nematode (*Heligmosomoides polygyrus,* Hp) and an apicomplexan protozoan (*Plasmodium yoelii,* Py). During single infections, Hp induced only mild disease symptoms. *Plasmodium* produced a substantial reduction in the number of red blood cells but all mice recovered from the infection. A different picture emerged in coinfected hosts. Hp maintained a profile of mostly asymptomatic infection when infecting hosts that had been previously infected with Py. On the contrary, Py incurred substantially higher costs in hosts that had been previously infected with Hp. We then investigated the possible reasons underlying the increase of Py virulence in hosts that had been previously infected with Hp. We found that coinfected hosts were less able to control Py multiplication and to recover from infection-induced anemia. Coinfected hosts had similar levels of erythropoietin and similar renewal of lost red blood cells compared to single Py infected hosts, resulting in decreased tolerance to Py infection. Experimental administration of erythropoietin in coinfected (Hp infecting first) hosts, partially decreased the severity of disease symptoms and improved tolerance. The detoxification of free heme released during the lysis of red blood cells, and the expression of Th1 and anti-inflammatory cytokine genes were also similar between coinfected and single infected hosts. However, coinfected mice had higher proportions of regulatory T cells expressing the CTLA-4 immune checkpoint, suggesting an enhanced immunosuppressive activity of Tregs. Py infection also induced the exhaustion of $CD8^+$ T cells, as coinfected mice had higher proportions of both $PD\text{-}1^+$ and $LAG\text{-}3^+$ $CD8^+$ T cells, and an increase in the $CD4^+/CD8^+$ ratio. Overall, these results stress the importance of the order of infection as a major determinant of malaria severity in hosts harboring a gastrointestinal nematode infection. We discuss the possible epidemiological and evolutionary consequences of these results.

44 *Keywords:* coinfection, helminths, *Plasmodium*, nematodes, virulence

45

Introduction

Coinfection is a widespread phenomenon in plants, wildlife, livestock and humans (Viney and Graham 2013), and describes the occurrence of different parasites/pathogens (hereafter we will use the term parasite as a general term) at the same time in the same individual host. Coinfection has the potential to change the two principal drivers of the infection dynamics, the within host multiplication and the between host transmission (Wait et al. 2021; Imrie et al. 2023), and therefore parasite fitness (Clay and Rudolf 2019) and virulence (i.e., infection-induced damage) (Alizon et al. 2013). During single infections, parasites might have a better access to host resources, while during coinfection, access to resources might be limited if competing parasites share the same infection site or consume the same host resources (Graham 2008; Griffiths et al. 2015). This might affect the within host multiplication rate (for parasites that do multiply within the host) and the transmission rate if coinfection reduces the number of propagules produced per unit of time. This bottom-up regulation of coinfecting parasites might also change the cost paid by the host (e.g., Szabo et al. 2024) if, for instance, the overall host resource consumption exceeds the consumption during single infections. In this case, parasite fitness can also be jeopardized if coinfection compromises the survival of the host. The regulation of the coinfection dynamics might also involve top-down mechanisms, where parasites strive to exploit the host in the face of the immune defenses deployed by the host (Graham 2008). Under this scenario, depending on the nature of the coinfecting parasites, coinfection can have protective [when, for instance, coinfecting parasites elicit similar immune effectors (Filbey et al. 2019)] or antagonistic effects on the host ability to clear the infection (Shen et al. 2019). Specifically, top-down regulation of coinfecting parasites might be compromised when different immune effectors are involved in the process of parasite clearance. Broadly speaking, this is usually the case when hosts are simultaneously infected with microparasites that elicit a Th1 immune response (e.g., viruses and protozoa) and macroparasites that induce a Th2 response (e.g., helminths) (Supali et al. 2010; Ezenwa and Jolles 2011; Ma et al. 2020).

71 Coinfection between micro and macroparasites is a public health issue in several countries of
72 the intertropical areas, given the high prevalence of helminthiases in humans and the overlap with the
73 endemicity of major infectious diseases, such as malaria or AIDS (Webb et al. 2012; Afolabi et al. 2021).
74 Coinfection between gastrointestinal helminths and malaria has attracted attention in the last decades
75 not only to understand if and how helminths might aggravate the severity of malaria symptoms
76 (Degarege et al. 2016; Kwan et al. 2018), but also to forecast the public health effect of deworming
77 campaigns on malaria incidence and severity (Fenton 2013; Budischak et al. 2018), or to assess the
78 potential effect of helminth infection on the efficacy of malaria vaccines (Su et al. 2006; Noland et al.
79 2010; Coelho et al. 2019). However, despite considerable effort, epidemiological studies overall report
80 an inconsistent pattern where coinfection can both result in protection or increased severity of malaria
81 symptoms (Nacher 2011; Salazar-Castañón et al. 2014; Degarege and Erko 2016). This inconsistency
82 can be explained by several factors related, for instance, to the species of coinfecting helminths
83 (Adegnika and Kremsner 2012; Hürlimann et al. 2019). Work conducted using animal models has also
84 reported inconsistent results, depending on mouse strains and parasite species (Segura et al. 2009;
85 Knowles 2011; Kolbaum et al. 2012). Here, we suggest that a previously underestimated factor shaping
86 the outcome of the coinfection might also be the order and timing of the infection with the two
87 parasites (Salazar-Castañón et al. 2018; Karvonen et al. 2019; Billet et al. 2020). In most epidemiological
88 studies, the order of infection is not taken into account because this information is typically not
89 available and might contribute to inflate the heterogeneity of the reported results.

90 The rationale underlying the hypothesis that order of infection is an important driver of the
91 coinfection dynamics rests on the observation that, when coinfecting parasites are regulated through
92 top-down effects, the polarization of the host immune response following the first infection (Hartgers
93 and Yazdanbakhsh 2006; Kotepui et al. 2023) makes the host more susceptible to a subsequent
94 infection with the second parasite (Su et al. 2005; Craig and Scott 2017). We explored this question
95 using a model of coinfection with the gastrointestinal nematode *Heligmosomoides polygyrus*
96 (hereafter Hp) and *Plasmodium yoelii* (hereafter Py) in mice. Hp is a model species in

97 immunoparasitology (Reynolds et al. 2012). This nematode is a natural parasite of rodents (Gregory et
98 al. 1992) which elicits a canonical Th2 immune response, orchestrated by Th2 cytokines, such as IL-4,
99 IL-5 and IL-13 (Reynolds et al. 2012). Mice are infected when ingesting infective larvae (L3), and adult
100 worms live in the lumen of the small intestine where they feed on the host's intestinal tissue (Bansemir
101 and Sukhdeo 1994). Py is also a model species for the study of the pathogenesis of malaria and the
102 associated immune response (Olatunde et al. 2022). The strain 17XNL of Py produces self-resolving
103 infections, and although the parasitemia can reach high level, all mice recover from the infection in
104 about four weeks. The cycle in the vertebrate host includes an early hepatic-stage that is followed by
105 the asexual replication within the red blood cells (RBCs) (blood-stage); the lysis of RBCs induces
106 anemia, the typical symptom of malaria infection. Infection with Py stimulates the production of pro-
107 inflammatory cytokines, such as the interferon-gamma (IFN-γ), and therefore polarizes the immune
108 response towards Th1 effectors (Olatunde et al. 2022).

109 Therefore, given that Hp and Py do not share the same ecological niche and do not share
110 common resources for their replication (RBCs for Py), or survival/reproduction (intestinal lumen for
111 Hp), any interference between the two parasites is unlikely to be driven by bottom-up regulation
112 mechanisms. On the contrary, given that the two parasites elicit different immune effectors, and that
113 Th1 and Th2 cytokines have reciprocal inhibitory effects (Paludan 1998), top-down mechanisms are
114 likely candidates to drive the outcome of the coinfection in this system.

115 We conducted a series of experiments with the aim of exploring to what extent the order and
116 timing of the infection with the two parasites drives the infection dynamics and the severity of the
117 disease. We also explored the possible mechanisms underlying the increased disease severity in
118 coinfected hosts. Based on the rationale reported above, we predicted that if the polarization of the
119 immune response towards Th1 (in the case of Py infection) or Th2 (in the case of Hp infection) makes
120 the host more vulnerable to the infection with the other parasite, coinfection should aggravate the
121 symptoms of the disease, compared to single infections.

122

123 **Materials and Methods**

124 *Ethical statement*

125 Experiments were approved by the Comité d'éthique Grand Campus Dijon of the University of
126 Burgundy and were authorized by the French Ministry of Higher Education and Research under the
127 numbers 33492 and 47573.

128 *Experimental animals and infections*

129 C57BL/6JRj female mice (7-10 weeks old) were purchased from Janvier Labs (Le Genest-Saint-
130 Isle, France), housed in cages containing 5 individuals under pathogen-free conditions, and maintained
131 under a constant temperature of 24°C and a photoperiod of 12h:12h light:dark with *ad libitum* access
132 to water and standard chow diet (A03-10, Safe, Augny, France). All mice were acclimatized to the
133 housing conditions during, at least, 7 days prior to the start of the experiments, were monitored twice
134 a day to check health status, and euthanized by cervical dislocation under anesthesia with isoflurane
135 either if they reached previously defined end points (and considered as mortality events in the survival
136 analysis) or at specific days post-infection (p.i.) for terminal collection of blood and organs (and
137 considered as censored events in the survival analysis).

138 Mice were infected with *Plasmodium yoelii* 17XNL by intra-peritoneal (i.p.) injection with $5x10^5$
139 infected red blood cells (iRBC) suspended in 0.1 ml of PBS and/or *Heligmosomoides polygyrus bakeri*
140 by oral gavage with L3 larvae (350 larvae suspended in 0.2 ml of drinking water).

141 *Experimental groups*

142 Mice were randomly assigned to 8 experimental groups as described in figure 1. A control
143 group (group 1) of mice was sham infected (i.p. injection of 0.1 ml of PBS and oral gavage with a 0.2
144 ml of drinking water). Two groups (groups 2 and 3) received single infections, either with Hp or Py. Five
145 additional groups were coinfected with the two parasites according to specific orders and timings of
146 infection. In one group, mice were simultaneously (same day) infected with the two parasites (group
147 4); in two groups, mice were infected first with Hp and subsequently with Py either at day 7 post Hp
148 infection, or at day 28 post Hp infection (groups 5 and 6); in two groups, mice were first infected with

149 Py and subsequently with Hp either at day 14 post Py infection, or at day 28 post Py infection (groups
150 7 and 8). The timings of infection in the coinfection groups correspond to specific stages in the life
151 cycles of the two parasites. Day 7 and 28 post Hp infection correspond to the stage that just precedes
152 the emergence of the adult worms in the intestinal lumen and when the infection has reached a
153 chronic stage, respectively. Day 14 and day 28 post Py infection approximately correspond to the
154 parasitemia peak and the end of the acute phase infection, respectively. The timings of the sequential
155 coinfection groups also correspond to the timing when the host immune response has been polarized
156 towards a Th2/Treg or a Th1 profile. For the simultaneous infection group, the two types of immune
157 response overlap during the early stage of the infection, with epithelial alarmin cytokines involved in
158 the Th2 response (Pelly et al. 2016, Xing et al. 2024) and NK and $\gamma\delta$ T cells producing Th1 cytokines
159 (IFN-γ, TNF-α) (Choudhury et al. 2000). The whole experiment was repeated twice (n_1 and n_2) with 40
160 mice per experimental group (n_1 = 20 and n_2 = 20), except for group 6 (n_1 = 17 and n_2 = 19) and group
161 8 (n_1 = 20 and n_2 = 15). However, not all traits were measured in all mice of the two replicates.

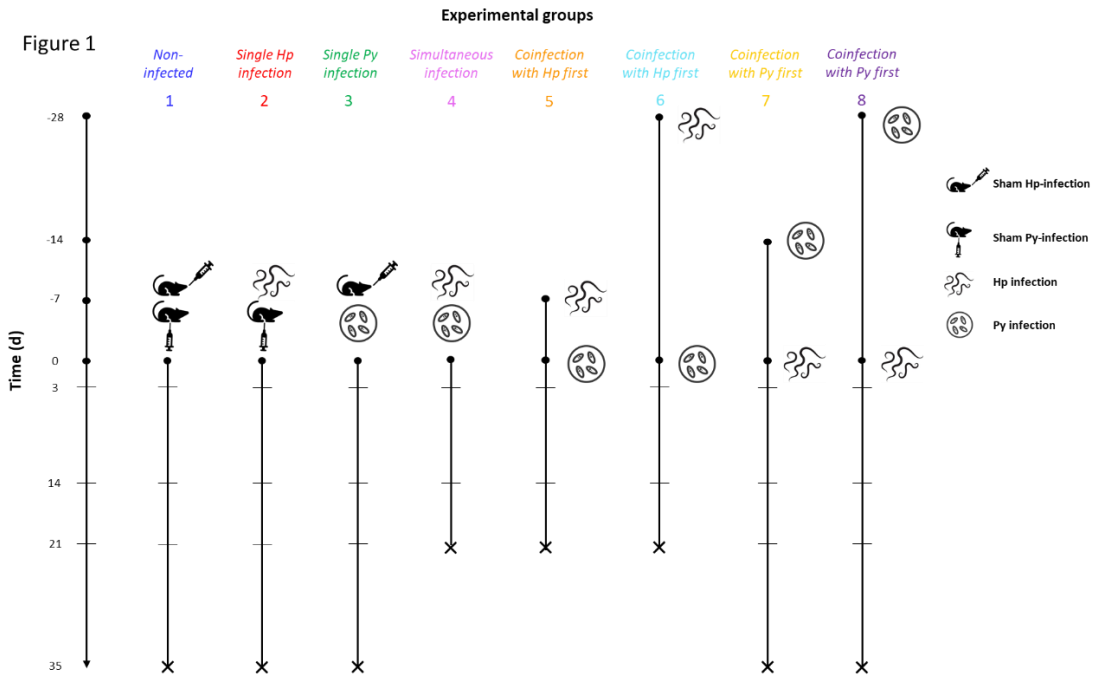

162

163 *Figure 1. Schematic view of the experimental setup and groups. Non-infected (group 1) and single (Hp,*
164 *Py) infected mice (groups 2 and 3) were monitored during 35 days post-infection. One group of*
165 *coinfected mice (group 4) was simultaneously (same day) infected with Py and Hp. The other coinfection*

166 *groups were either infected first with Hp (at day -7 or day -28) and then with Py at day 0 (groups 5 and*
167 *6), or infected first with Py (at day -14 or day -28) and then with Hp at day 0 (groups 7 and 8). Groups*
168 *4, 5 and 6 were monitored during 21 days post last exposure. We used a color code to distinguish the*
169 *different experimental groups: 1 = blue, 2 = red, 3 = green, 4 = magenta, 5 = dark orange, 6 = deep sky*
170 *blue, 7 = gold, 8 = violet. These color codes were consistently used in all subsequent figures.*
171
172 *Erythropoietin administration*
173 Mice (n = 20) were infected with Hp and at day 28 p.i. they were infected with Py. Mice were
174 then split randomly into two groups, one received an i.p. injection of 1 µg of recombinant mouse
175 erythropoietin (rEPO) (959-ME, Bio-Techne, Minneapolis, Minnesota, USA) in 200 µl of PBS at days 0,
176 2 and 4 post Py infection; the other group was injected with 200 µl of PBS only, for control.
177 *Monitoring of health status, hematological and plasma parameters, and Py parasitemia*
178 Mice were regularly weighed (at least three times a week) and body mass was used as an
179 integrative marker of host health. Hematological parameters were assessed by collecting 10 µl of blood
180 from the tail tip in 0.5 ml tubes with 1 µl of heparin (Héparine Choay® 25 000 UI/5ml, Sanofi-Aventis,
181 Gentilly, France). These samples were immediately read with a SCIL Vet abc Plus+ hematology analyzer
182 (Horiba Medical, Montpellier, France) to assess RBC counts and mean globular volume (a proxy of
183 reticulocyte production). For mice with Py infection, a drop of blood was smeared on a slide and fixed
184 with methanol. Slides were subsequently stained with a Giemsa RS solution (Carlo Erba Reagents, Val
185 de Reuil, France) (10% v/v in phosphate buffer) for 15 minutes and rinsed with water. Infected RBCs
186 were counted using an optical microscope under magnification x1000, and parasitemia expressed as
187 the proportion of iRBCs.
188 At day 3, 14, 21 and 35 p.i. (post last infection for the coinfection groups), five mice per group
189 were euthanized by cervical dislocation under isoflurane anesthesia, for terminal collection of total
190 peripheral blood and organs. Given the severity of the disease symptoms, the simultaneous infection
191 group and the two coinfection groups first infected with Hp (groups 4, 5, 6) were only monitored up to

192 day 21 post last infection. Plasma was separated from total blood by centrifugation (7 min 3000 rpm
193 4°C), aliquoted and stored at -80°C.

194 Plasma levels of aspartate aminotransferase (AST) and heme oxygenase-1 (HO-1) were
195 assessed with ab263882 and ab229431 commercial ELISA kits from Abcam (Cambridge, UK),
196 respectively, with the aim of investigating infection-induced liver damage (AST) and the scavenging of
197 free heme groups released during the lysis if RBCs (HO-1). Plasma levels of mouse erythropoietin (EPO)
198 were assessed with EM28RB commercial ELISA kit from Invitrogen™ (Carlsbad, California, USA). Plates
199 were read with a SpectraMax iD3 multi-mode microplate reader (Molecular Devices, San Jose,
200 California, USA).

201 *Organ collection*

202 Spleen was removed and weighed. About one third of the spleen was cut and immediately
203 frozen in liquid nitrogen for RT-qPCR, and the remaining was kept on ice in PBS before the flow
204 cytometry staining procedure. A liver slice (left lobe) was also immediately frozen in liquid nitrogen for
205 RT-qPCR.

206 *RNA extraction and qPCR for Hmox-1, IFN-γ, IL-10 and TGF-β1 gene expression*

207 Tissues were homogenized in TRIzol™ Reagent (Invitrogen™, Carlsbad, California, USA) under
208 strong agitation using 0.5 mm glass beads and a Precellys® 24 Touch homogenizer (Bertin
209 Technologies, Montigny-le-Bretonneux, France). RNA extraction was performed following the
210 manufacturer's instructions. RNA concentration was measured with a NanoPhotometer® N50 (Implen,
211 Munich, Germany). Reverse transcription was performed with a High-Capacity cDNA Reverse
212 Transcription Kit (Applied Biosystems™, Foster City, California, USA) from 1.5 µg total RNA.
213 Quantitative PCR was performed with PowerUp™ SYBR™ Green Master Mix (Applied Biosystems™) on
214 a QuantStudio™ 3 Real-Time PCR System (Applied Biosystems™). We used two housekeeping genes (β-
215 actin and GAPDH); β-actin provided more consistent values (less intra-group variability) and therefore
216 we used it as the reference gene (i.e., the level of expression of the genes of interest relative to the
217 expression of the housekeeping gene). Primer sequences are reported in the supplementary material

218 (table S1), and were checked for specificity using the Primer-BLAST tool (NCBI). Melt curve analysis was
219 also performed in all samples to check for the presence of nonspecific amplification products.

220 *Assessment of immune cell populations through spectral flow cytometry*

221 Spleens were homogenized with a 70 µm cell strainer and washed twice with PBS to obtain a
222 single-cell suspension. RBCs were removed from suspensions with eBioscience™ RBC Lysis Buffer
223 (Invitrogen™) (3 min incubation at RT). Cells were counted with viability trypan blue dye and
224 dispatched in 96-well V bottom plates to obtain $1x10^7$ live cells/well. Cells were then stained with
225 LIVE/DEAD™ Fixable Blue Dead Cell Stain Kit (Invitrogen™) in PBS for 30 min at 4°C, incubated in stain
226 buffer with BD Fc Block™ (BD Pharmingen™, Franklin Lakes, New Jersey, USA) for 15 min at RT (0.5
227 µg/well), and stained with surface antibodies in brilliant stain buffer (see table S2 for details on the
228 markers used) for 30 min at 4°C. Cells were then fixed and permeabilized with eBioscience™ Foxp3 /
229 Transcription Factor Staining Buffer Set (Invitrogen™) prior intracellular staining in brilliant stain buffer
230 (table S2) for 30 min at RT. Cells were resuspended in stain buffer, filtered with 100 µm nylon mesh
231 and analyzed on a 4-lasers (UV/V/B/R) Aurora™ (Cytek® Biosciences, Fremont, California, USA) spectral
232 flow cytometer in the ImaFlow Facility, part of the US58 BioSanD. Events were gated and analyzed with
233 SpectroFlo® v3.0.0 software (Cytek® Biosciences) (see figures S1 and S2 for the gating strategy).

234 *Statistical analyses*

235 We used general and generalized linear mixed models (GLMM) to analyze data where each
236 individual mouse was repeatedly sampled, using either a normal distribution or a beta distribution (i.e.,
237 for proportions) of errors. Mouse ID was included in these models as a random intercept. Variables do
238 not necessarily vary linearly with time over the course of the infection. We therefore included squared
239 (and cubic) time p.i. to capture these nonlinear relationships. However, polynomial regression might
240 provide a poor fit to the data. Therefore, we also ran general additive models (GAM) where the degrees
241 of freedom of the smoothing function were chosen based on the generalized cross-validation (GCV)
242 optimization criterion. Some variables had an asymmetrical distribution and were log-transformed to
243 reduce skewness and meet the model assumptions.

244 Differences in survival between groups were analyzed using the Kaplan Meier estimator and
245 significance assessed using a Log-Rank test. For coinfected mice, any mortality that had occurred
246 before the infection with the second parasite was considered as caused by single infections (and
247 therefore included as single infected individuals in the model); any effect of coinfection on survival
248 was, thus, assessed only after the infection with the second parasite. To increase the statistical power,
249 the survival analysis also included additional mice that were followed for a longer period of time (up
250 to day 99 p.i.) to assess the long-term effect of coinfection on the infection dynamics. These mice, that
251 involved all the infection groups (excluding therefore the non-infected individuals), were housed in the
252 same conditions and received the same infection protocols (dose, timing of the infection), the only
253 difference being that they were not euthanized at specific time points (unless they reached the end
254 points). Therefore, the survival analysis included up to four replicated datasets for the infection groups
255 and two replicated datasets for the non-infected group.

256 For variables that were measured only once per individual mouse (spleen mass, AST, EPO, gene
257 expressions, HO-1, and immune cell population by flow cytometry), we ran general or generalized
258 linear models (GLM), depending on the distribution of errors (normal or beta distribution). Post-hoc
259 comparisons between groups were done using LS-means with Bonferroni correction of p values.

260 Differences in sample size across groups reflect missing values, either due to the reaching of
261 the end point or to technical issues during the processing of the sample.

262 To simplify the interpretation of the results, we ran different sets of models, comparing
263 different groups. First, we compared non-infected mice versus single infections (groups 1, 2 and 3).
264 These models provided us with the baseline information on the intrinsic effect of each parasite when
265 infecting the host alone. Then, we compared single infections versus coinfection groups. This was done
266 separately for Py and Hp by including in the model the corresponding coinfection groups where Py and
267 Hp infected mice that had been previously infected with the other parasite (i.e., groups 3, 4, 5, 6 in one
268 model, and groups 2, 7, 8 in another model). The simultaneous infection group (group 4) was always
269 included in the Py model. Given that the timing of the infection did appear to have minor effects on

270 the response variables, we also ran models where the different coinfection groups were clustered
271 together (groups 4, 5 and 6 together; groups 7 and 8 together) and we compared non-infected, single
272 infected and coinfected hosts in the same model. Finally, we ran a model that was restricted to the
273 sequential coinfection groups (excluding the simultaneous infection group) where we could assess the
274 effect of the order of the infection [either Hp first (groups 5 and 6), or Py first (groups 7 and 8)]. All the
275 statistical analyses and figures were done using SAS Studio.

276 **Results**

277 ***Severity of the disease in single and coinfected hosts***

278 *Body mass*

279 We analyzed body mass as percent change relative to the body mass at the day of the sham-
280 infection for the control group (group 1) and the day of the infection for single and simultaneous
281 infection groups (groups 2, 3 and 4) or the day of the last infection for the sequential coinfection groups
282 (groups 5, 6, 7 and 8) (corresponding to t = 0 in fig. 1). We first compared changes in body mass over
283 time between non-infected and single (Hp, Py) infected mice (groups 1, 2, 3). The model showed that
284 body mass increased linearly over time, at a similar rate for non-infected and single infected mice
285 (table 1, fig. 2a).

286

287 *Table 1. General linear mixed model investigating the changes in body mass (percent change with*
288 *respect to day 0) in non-infected and single (Hp and Py) infected mice. We report the parameter*
289 *estimates with the 95% CI, degrees of freedom (df), F and p values. Mouse ID was included as a random*
290 *effect to take into account the non-independence of observations for the same individual over time. N*
291 *= 120 individuals and 774 observations.*

Fixed effects		**Estimate**	**95% CI**	**df**	**F**	**p**
Treatment				2,648	0.24	0.7828
	non-infected	0				
	single Hp	-0.47	-3.13/2.20			
	single Py	-0.95	-3.60/1.71			
Time		0.54	0.35/0.74	1,648	83.44	<0.0001
Squared time		-0.004	-0.01/0.001	1,648	2.80	0.095
Time*Treatment				2,648	0.12	0.8827
	non-infected	0				
	single Hp	0.007	-0.27/0.29			
	single Py	-0.06	-0.33/0.22			
Squared Time*Treatment				2,648	0.88	0.4141
	non-infected	0				
	single Hp	0.0003	-0.01/0.01			
	single Py	0.005	-0.003/0.01			
Random effect		**Estimate**	**SE**	**z**	**P**	
ID		16.49	2.49	6.62	<0.0001	

292

293 We then compared changes in body mass in mice that were infected with Py alone and mice
294 that were simultaneously infected or were first infected with Hp and then with Py (groups 4, 5, 6).
295 Although mice in the coinfection groups lost body mass from day 14 post Py infection onwards (table
296 S3, fig. S3a), the squared time by treatment interaction was not statistically significant (table S3). Given
297 that there was no apparent difference in the dynamics of body mass change between the coinfection
298 groups, we ran an additional model where we compared the changes in body mass between non-
299 infected, single Py infected and coinfected groups (groups 4, 5 and 6 together). This model showed a
300 strong effect of coinfection on changes in body mass (table 2, fig. 2b), with coinfected mice losing body
301 mass over the course of the infection.

302

303

304

305 *Table 2. General linear mixed model investigating the changes in body mass (percent change with*
306 *respect to day 0) in non-infected, single Py infected and coinfected (simultaneous infection and Hp*
307 *infecting first) mice. We report the parameter estimates with the 95% CI, degrees of freedom (df), F*
308 *and p values. Mouse ID was included as a random effect to take into account the non-independence of*
309 *observations for the same individual over time. N = 196 individuals and 1009 observations.*

Fixed effects		**Estimate**	**95% CI**	**df**	**F**	**P**
Treatment				2,807	3.0	0.0503
	non-infected	0				
	single Py	-4.50	-8.2/-0.8			
	coinfection (groups 4,5,6)	-1.55	-4.6/1.5			
Time		0.60	0.14/1.06	1,807	76.87	<0.0001
Squared time		-0.01	-0.03/0.01	1,807	56.88	<0.0001
Time*Treatment				2,807	3.57	0.0285
	non-infected	0				
	single Py	0.88	0.23/1.53			
	coinfection (groups 4,5,6)	0.47	-0.07/1.01			
Squared Time* Treatment				2,807	9.72	<0.0001
	non-infected	0				
	single Py	-0.04	-0.07/-0.01			
	coinfection (groups 4,5,6)	-0.05	-0.07/-0.03			
Random effect		**Estimate**	**SE**	**Z**	**p**	
ID		16.7	2.1	7.95	<0.0001	

310

311 A different picture emerged when comparing changes in body mass in mice that were infected
312 first with Py and then with Hp (groups 7 and 8). In this case, coinfection slowed down the rate of body
313 mass gain, but did not produce a loss in body mass (table S4, fig. S3b). As the timing of infection did
314 not have any effect on the changes in body mass, we grouped them and ran an overall model
315 comparing non-infected, single Hp infected and coinfected groups (7 and 8 together). This model
316 confirmed the slight effect of coinfection on the dynamics of body mass change, with coinfected mice
317 having a slower rate of increase in body mass, but not losing mass over time (table 3, fig. 2c). Finally,
318 we ran a model that was only restricted to the four sequential coinfection groups (groups 5, 6, 7 and
319 8), excluding the simultaneous infection group. This model confirmed to importance of the order of
320 infection in shaping the dynamics of body mass (table S5, fig. 2d).

321

322

323

324 *Table 3. General linear mixed model investigating the changes in body mass (percent change with*
325 *respect to day 0) in non-infected, single Hp infected and coinfected (Py infecting first) mice. We report*
326 *the parameter estimates with the 95% CI, degreed of freedom (df), F and p values. Mouse ID was*
327 *included as a random effect to take into account the non-independence of observations for the same*
328 *individual over time. N = 155 individuals and 869 observations.*

Fixed effects		**Estimate**	**95% CI**	**df**	**F**	**p**
Treatment				2,708	1.06	0.3477
	non-infected	0				
	single Hp	-0.52	-2.61/1.57			
	coinfection (groups 7,8)	0.8	-1.042.64			
Time		0.54	0.40/0.68	1,708	86.46	<0.0001
Squared time		-0.004	-0.008/-0.0005	1,708	0.58	0.4468
Time* Treatment				2,708	22.19	<0.0001
	non-infected	0				
	single Hp	0.007	-0.2/0.21			
	coinfection (groups 7,8)	-0.52	-0.70/-0.34			
Squared Time* Treatment				2,708	9.50	<0.0001
	non-infected	0				
	single Hp	0.0007	-0.005/0.006			
	coinfection (groups 7,8)	0.01	0.005/0.015			
Random effect		**Estimate**	**SE**	**z**	**P**	
ID		11.96	1.62	7.37	<0.0001	

329

330

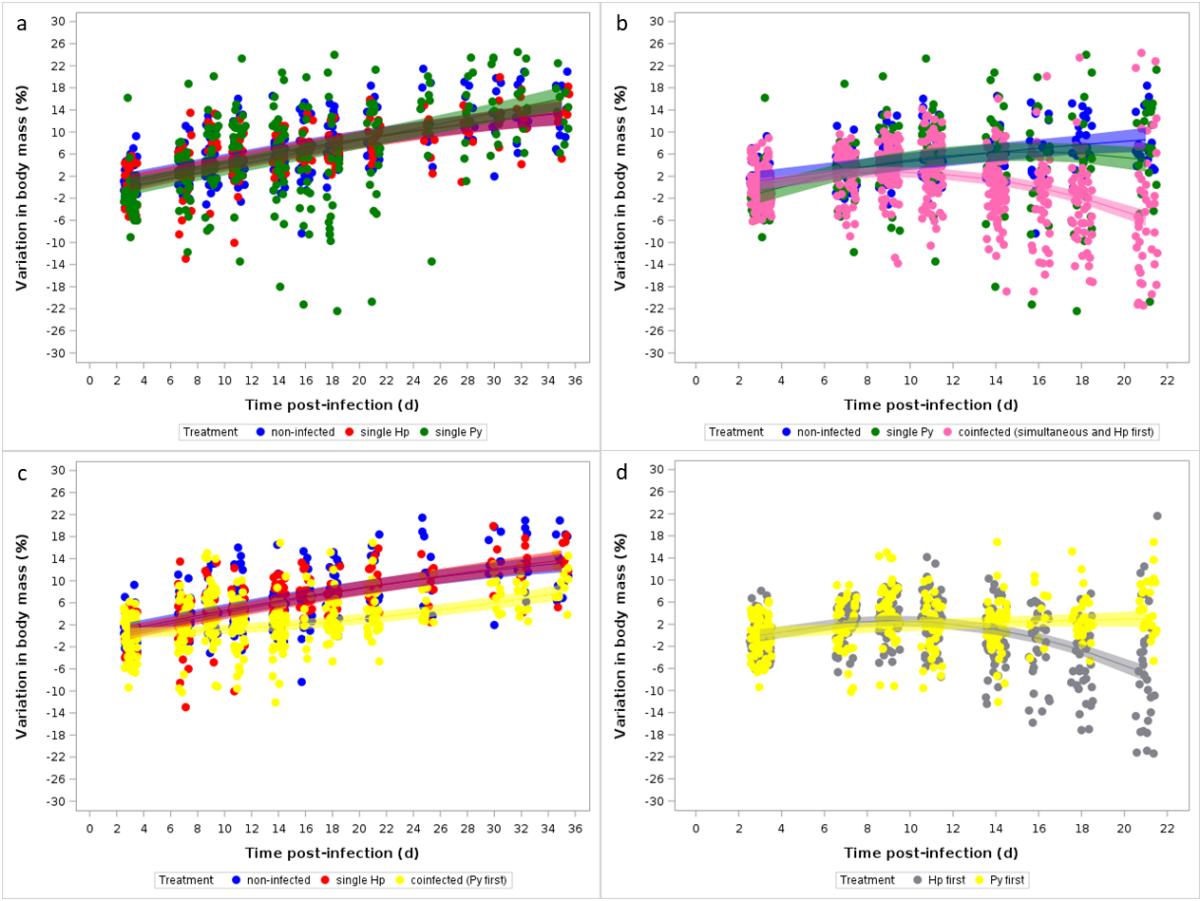

Figure 2. Changes in body mass over the course of the infection. Body mass is expressed as percent change with respect to body mass at day 0 [for the non-infected, single (Hp, Py) infected, and simultaneous infection groups] or at the day of the last infection for the sequential coinfection groups. a) Changes in body mass for non-infected and single (Hp, Py) infected mice; b) Changes in body mass for non-infected, single Py infected and coinfected (simultaneous infection Hp infecting first) groups; c) Changes in body mass for non-infected, single Hp infected and coinfected (Py infecting first) groups; d) Changes in body mass for coinfected groups depending on the order of the infection (Hp infecting first or Py infecting first). Dots represent the raw data, the lines represent the fit of a GLMM, and the shaded area around the line the 95% CI.

Therefore, coinfection aggravated one of the most integrative symptoms of disease severity, but the magnitude of the aggravating effect was strongly dependent on the order of the infection, being greatest in mice that were infected with Hp first.

345 *Splenomegaly*

346 Splenomegaly (i.e., the enlargement of the spleen) is another prominent symptom of the
347 infection with Hp or Py. We measured spleen mass at day 3, 14, 21 and 35 p.i. and confirmed that
348 single infection induced splenomegaly of different magnitude depending on the parasite, with larger
349 spleen mass in Py infected mice, especially at day 14 – 21 p.i. (table S6, fig. S4a). When comparing
350 groups infected first with Hp and then with Py (plus the simultaneous infection, groups 4, 5, 6),
351 coinfection only had a mild initial effect on splenomegaly at day 3 post Py infection compared to single
352 Py infected hosts (Table S7), but by day 14 p.i. the differences vanished (fig. S5a). This result was
353 corroborated when comparing non-infected, single Py infected and coinfected groups together (Table
354 S8, fig. S4b).

355 When comparing the effect of coinfection in groups that were first infected by Py (groups 7
356 and 8), we found only a moderate increase in spleen mass, essentially as a consequence of the residual
357 enlargement due to the previous Py infection, since the difference between single Hp infection and
358 coinfection groups tended to vanish over time (table S9 and table S10, fig. S4c, fig. S5b).

359 The asymmetric effect of infection order on splenomegaly was best captured by the model on
360 the four sequential coinfection groups (groups 5, 6, 7 and 8) where mice were either infected first with
361 Hp or with Py. This model showed that spleen mass increased over the course of the infection only
362 when mice were first infected with Hp (table S11, fig. S4d).

363 Therefore, as for body mass, coinfection affected splenomegaly in an asymmetric way,
364 depending on infection order, with larger spleens in mice infected first with Hp and subsequently with
365 Py.

366 *Marker of liver damage*

367 We compared a marker of liver damage (aspartate aminotransferase, AST) in plasma at day 21
368 p.i. in non-infected and single (Hp, Py) infected mice, and found that Py infected mice had moderately
369 higher levels of AST compared to non-infected hosts (GLM, $F_{2,23} = 4.45$, $p = 0.0218$, $n = 26$ individuals;
370 fig. S6a). Coinfection did aggravate liver damage in the groups where Py followed the Hp infection (plus

371 simultaneous infection, groups 4, 5, 6) (GLM, $F_{3,36} = 4.28$, $p = 0.0111$, $n = 40$; fig. S7a), and this effect
372 was confirmed when analyzing non-infected, single Py infected and coinfected mice together in the
373 same model (GLM, $F_{2,45} = 4.22$, $p = 0.0209$, $n = 48$; fig. S6b).

374 We found rather similar effects of coinfection when analyzing the groups where Hp follows Py
375 (groups 7 and 8), with coinfection groups having higher AST levels compared to non-infected and single
376 Hp infected groups (GLM, $F_{2,29} = 4.96$, $p = 0.0141$, $n = 32$; fig. S6c, fig. S7b). As a consequence, there
377 was no effect of infection order in the coinfection groups (groups 5, 6, 7 and 8) on AST level at day 21
378 p.i. (GLM, $F_{1,35} = 0.28$, $p = 0.5976$, $n = 37$; fig. S6d).

379 Therefore, coinfection tended to aggravate liver damage with no effect of infection order.

380 *Survival*

381 In agreement with the pattern of change in body mass over the course of the infection, we did
382 not find any difference in the survival rate between non-infected and single infected mice (Log-Rank
383 test $\chi^2_2 = 0.92$, $p = 0.6315$, $n = 229$; fig. 3a). Single Py infected mice had higher survival compared to
384 the simultaneous infection and coinfection groups (groups 4, 5 and 6) (Log-Rank test $\chi^2_3 = 22.81$, $p <$
385 0.0001, $n = 242$, fig. S8), but there was no difference according to the timing of coinfection (all sidak-
386 adjusted p values > 0.6. We therefore compared the coinfection groups together with the non-infected
387 and single Py infected and found a strong effect of coinfection (Log-Rank test $\chi^2_2 = 26.02$, $p < 0.0001$,
388 $n = 282$; fig. 3b).

389 There was no host mortality in the coinfection groups where Hp followed Py (groups 7 and 8).
390 Therefore, there was no difference in the mortality rate of non-infected, single Hp infected and
391 coinfected groups (groups 7 and 8) (Log-Rank test $\chi^2_2 = 2.34$, $p = 0.3099$, $n = 229$; fig. 3c). As a
392 consequence, order of infection was a strong predictor of host mortality in the sequential coinfection
393 groups (groups 5, 6, 7 and 8) (Log-Rank test $\chi^2_1 = 13.47$, $p = 0.0002$, $n = 189$; fig. 3d).

394 Overall, these results show that order of infection has a paramount effect on the severity of
395 the symptoms and therefore on parasite virulence (infection-induced damage), with Hp infection
396 producing mild symptoms whatever the order of the infection, and Py becoming substantially more

397 virulent when infecting hosts already harboring the nematode. However, the timing of infection had

398 virtually no effect on disease severity.

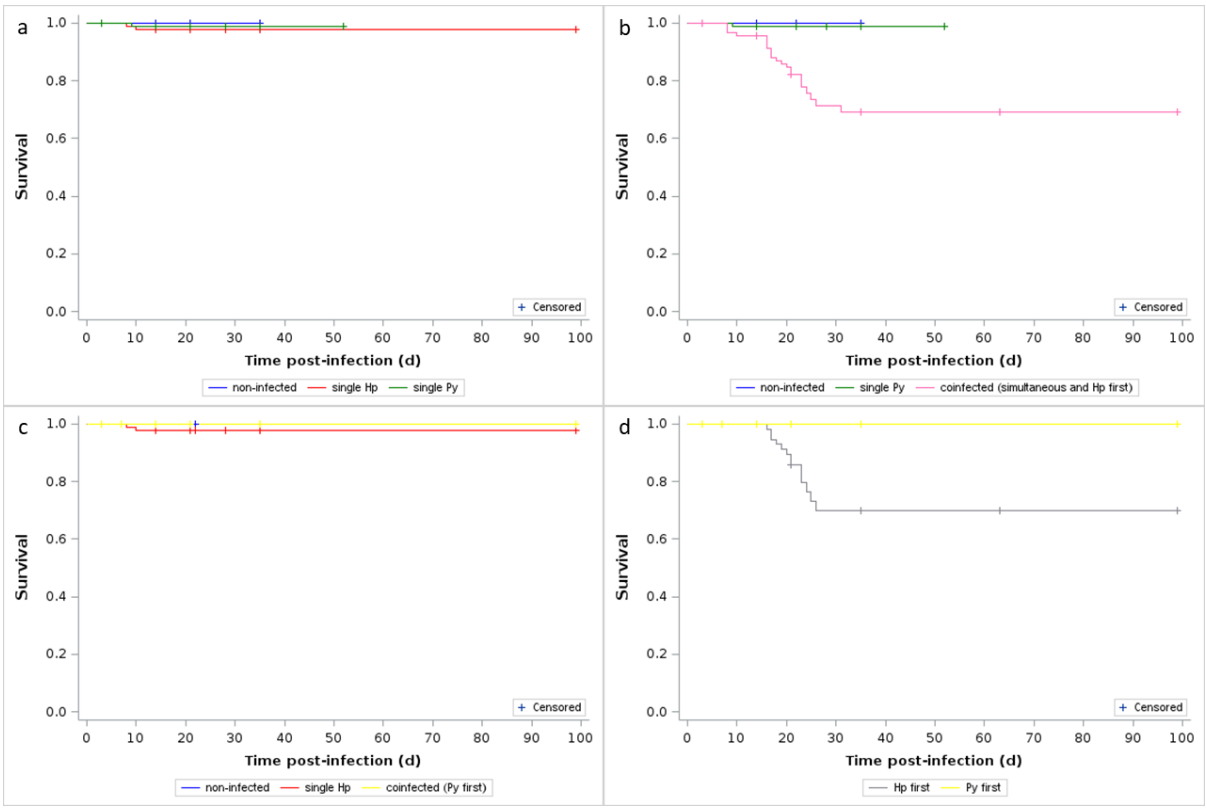

399

400 *Figure 3. Effect of infection and coinfection on host survival. a) Survival curves for non-infected and*

401 *single (Hp, Py) infected mice; b) Survival curves for non-infected, single Py infected and coinfected*

402 *(simultaneous infection and Hp first) mice; c) Survival curves for non-infected, single Hp infected and*

403 *coinfected (Py infecting first) mice; d) Survival curves for coinfected mice depending on the order of*

404 *infection (Hp infecting first or Py infecting first). Crosses indicate censored observations.*

405

406 ***Parasitemia***

407 If previous infection with Hp makes the host more susceptible to a subsequent Py infection,

408 we should expect higher parasitemia in coinfected hosts (groups 4, 5, 6) compared to single Py

409 infection. During single Py infection, parasitemia reached a peak at around day 16 p.i., and then the

410 infection resolved by day 30 (fig. 4a; fig. S9). Given that the coinfection groups (groups 4, 5 and 6) were

411 stopped at day 21 p.i., we could only compare the rising and the early declining stages of the

412 parasitemia. The model showed that coinfected groups reached higher parasitemia and that, contrary

413 to the single Py infection group, the parasitemia of coinfected mice kept increasing up to day 21 p.i.
414 (table S12 and table 4, fig. S10 and fig. 4b).
415
416 *Table 4. General linear mixed model investigating the changes in parasitemia (proportion of iRBC) in*
417 *single Py infected and coinfected (simultaneous infection and Hp first) hosts. We report the parameter*
418 *estimates with the 95% CI, degrees of freedom (df), F and p values. Mouse ID was included as a random*
419 *effect to take into account the non-independence of observations for the same individual over time.*
420 *The distribution of errors was modelled using a beta distribution. N = 151 individuals and 665*
421 *observations.*

Fixed effects		**Estimate**	**95% CI**	**df**	**F**	**p**
Treatment				1,510	11.3	0.0008
	single Py	0				
	coinfection (groups 4, 5, 6)	1.95	0.81/3.1			
Time		1.05	0.9/1.2	1,510	428.25	<0.0001
Squared time		-0.03	-0.04/0.02	1,510	230.38	<0.0001
Time*Treatment				1,510	12.12	0.0005
	single Py	0				
	coinfection (groups 4, 5, 6)	-0.3	-0.48/-0.13			
Squared Time*Treatment				1,510	17.63	<0.0001
	single Py	0				
	coinfection (groups 4, 5, 6)	0.01	0.007/0.019			
Random effect		**Estimate**	**SE**	**z**	**p**	
ID		0.139	0.032	4.32	<0.0001	

422
423 Therefore, as expected, previous or simultaneous infection with Hp increased host
424 susceptibility to a subsequent infection, since Py replicated more and for longer time in coinfected
425 mice. Enhanced persistent parasitemia might thus explain the observed increase of Py virulence in
426 coinfected hosts through specific costs incurred during the asexual reproduction of Py.
427
428

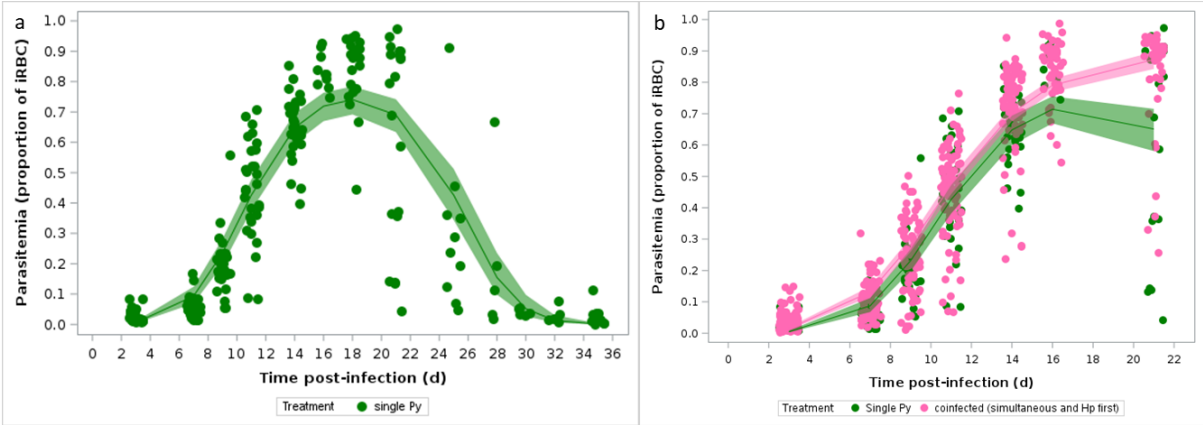

Figure 4. Changes in parasitemia over the course of the infection. a) Changes in parasitemia (proportion of iRBCs counted using optical microscopy) in single Py infected mice over time; b) Changes in parasitemia (proportion of iRBCs) in single Py infected and coinfected (simultaneous infection and Hp first) mice. Dots represent the raw data, the lines represent the fit of the GLMM, and the shaded area around the line the 95% CI.

Specific costs of Py infection

The principal cost induced by Py infection is related to the anemia caused by the lysis of RBCs during the asexual reproduction of the parasite (Olatunde et al. 2022). We therefore assessed the changes in RBC counts over the course of the infection. First, we compared changes in RBC counts between non-infected and single (Hp, Py) infections. As expected, Py infection produced a sharp decline in the number of RBCs, while there was no difference between non-infected and single Hp infection (table 5, fig. 5a, fig. S11), corroborating the idea that Py and Hp do not compete for common resources.

450 *Table 5. General linear mixed model investigating the changes in RBC counts (10^6/µl) in non-infected*
451 *and single (Hp, Py) infected mice. We report the parameter estimates with the 95% CI, degrees of*
452 *freedom (df), F and p values. Mouse ID was included as a random effect to take into account the non-*
453 *independence of observations for the same individual over time. N = 60 individuals and 360*
454 *observations.*

Fixed effects		**Estimate**	**95% CI**	**df**	**F**	**p**
Treatment				2,291	5.27	0.0056
	non-infected	0				
	single Hp	0.709	0.101/1.361			
	single Py	0.967	0.36/1.574			
Time		-0.224	-0.35/-0.098	1,291	197.56	<0.0001
Squared time		0.013	0.003/0.023	1,291	86.17	<0.0001
Cubic time		-0.0002	-0.0004/-5^{e-6}	1,291	39.83	<0.0001
Time*Treatment				2,291	36.27	<0.0001
	non-infected	0				
	single Hp	-0.163	-0.344/0.017			
	single Py	-0.735	-0.913/-0.557			
Squared time*Treatment				2,291	9.55	<0.0001
	non-infected	0				
	single Hp	0.011	-0.003/0.025			
	single Py	0.031	0.017/0.045			
Cubic time*Treatment				2,291	2.22	0.1101
	non-infected	0				
	single Hp	-0.0002	-0.0005/0.00008			
	single Py	-0.0003	-0.0006/-0.00001			
Random effect		**Estimate**	**SE**	**z**	**P**	
ID		0.1415	0.061	2.37	0.0089	

455

456 Coinfected groups (groups 4, 5, 6) had a similar drop in the count of RBCs (table S13, fig.
457 S12a,b), and we clustered them and compared the changes in RBC counts between non-infected, single
458 Py infected and coinfected mice (groups 4, 5, 6). The model showed that coinfected mice still had low
459 levels of RBCs at day 21 p.i. compared to single Py infected mice that had already started the recovery
460 phase (table 6, fig. 5b, fig. S12c).

461

462

463

464

465

466 *Table 6. General linear mixed model investigating the changes in RBC count (10^6/µl) in non-infected,*
467 *single Py infected and coinfected (simultaneous infection and Hp first) mice. We report the parameter*
468 *estimates with the 95% CI, degreed of freedom (df), F and p values. Mouse ID was included as a random*
469 *effect to take into account the non-independence of observations for the same individual over time. N*
470 *= 94 individuals and 476 observations.*

Fixed effects		**Estimate**	**95% CI**	**df**	**F**	**p**
Treatment				2,373	1.70	0.1840
	non-infected	0				
	single Py	0.263	-0.40/0.92			
	coinfected (groups 4, 5, 6)	-0.24	-0.79/0.31			
Time		-0.074	-0.29/0.14	1,373	0.03	0.8556
Squared time		-0.006	-0.032/0.021	1,373	67.42	<0.0001
Cubic time		0.0004	-0.0004/0.001	1,373	108.37	<0.0001
Time*Treatment				2,373	0.73	0.4826
	non-infected	0				
	single Py	0.166	-0.14/0.471			
	coinfected (groups 4, 5, 6)	0.024	-0.23/0.28			
Squared Time*Treatment				2,373	11.62	<0.0001
	non-infected	0				
	single Py	-0.09	-0.127/-0.052			
	coinfected (groups 4, 5, 6)	-0.057	-0.088/-0.026			
Cubic Time*Treatment				2,373	17.96	<0.0001
	non-infected	0				
	single Py	0.004	0.002/0.005			
	coinfected (groups 4, 5, 6)	0.002	0.001/0.003			
Random effect		**Estimate**	**SE**	**z**	**P**	
ID		0.37	0.084	4.37	<0.0001	

471

472 Infection-induced anemia stimulates erythropoiesis with the aim of restoring homeostatic RBC
473 counts. We therefore investigated whether coinfection impaired the host capacity to repair the
474 damage (here the loss of RBCs) caused by the infection. To this purpose, we assessed the production
475 of erythropoietin (EPO) (at day 14 and 21 p.i.) and the mean globular volume (MGV) that, in the case
476 of malaria-induced anemia, reflects the proportion of reticulocytes among the total RBCs.

477 Mice with single Py infection produced EPO in response to the loss of RBCs compared to non-
478 infected individuals (GLM, $F_{1,34}$ = 113.53, p < 0.0001, n = 38; fig. 5c). However, despite having lower
479 RBC counts, coinfected hosts (groups 4, 5, 6) did not produce more EPO compared to single Py infected
480 mice, neither when including each coinfection group separately in the model (GLM, $F_{3,67}$ = 2.24, p =
481 0.0917, n = 75; fig. S13), nor when grouping them (post hoc comparison of LS-means between single
482 infection and coinfection with Bonferroni correction, p = 0.3096, n = 94; fig. 5c)

483 This result was mirrored by the change of MGV over the course of the infection. Py infected
484 mice had a sharp increase in the MGV between day 11 and 21 p.i., compared to non-infected and Hp
485 infected mice, indicating a higher proportion of reticulocytes among RBCs (table 7, fig. 5d, fig. S14).
486 However, changes in MGV were similar between single Py infection and the coinfection groups (groups
487 4, 5, 6) (table 8, fig. 5e, table S14, fig. S15).
488
489 *Table 7. General linear mixed model investigating the changes in mean globular volume (fL) in non-*
490 *infected and single (Hp, Py) infected mice. We report the parameter estimates with the 95% CI, degrees*
491 *of freedom (df), F and p values. Mouse ID was included as a random effect to take into account the*
492 *non-independence of observations for the same individual over time. N = 60 individuals and 360*
493 *observations.*

Fixed effects		**Estimate**	**95% CI**	**df**	**F**	**p**
Treatment				2,291	1.90	0.151
	non-infected	0				
	single Hp	0.658	-2.108/3.424			
	single Py	-1.975	-4.738/0.789			
Time		0.486	-0.09/1.061	1,291	8.14	0.0046
Squared time		-0.026	-0.071/0.02	1,291	0.94	0.3326
Cubic time		0.0003	-0.0006/0.001	1,291	8.0	0.005
Time*Treatment				2,291	3.20	0.0423
	non-infected	0				
	single Hp	-0.529	-1.354/0.295			
	single Py	0.53	-0.284/1.343			
Squared Time*Treatment				2,291	3.37	0.0358
	non-infected	0				
	single Hp	0.032	-0.033/0.097			
	single Py	0.084	0.02/0.148			
Cubic Time*Treatment				2,291	10.55	<0.0001
	non-infected					
	single Hp	-0.0005	-0.002/0.0008			
	single Py	-0.003	-0.004/-0.002			
Random effect		**Estimate**	**SE**	**z**	**P**	
ID		2.86	1.18	2.42	0.0078	

494
495
496
497
498
499

500 *Table 8. General linear mixed model investigating the changes in mean globular volume (fL) in non-*
501 *infected, single Py infected and coinfected (simultaneous infection and Hp first) mice. We report the*
502 *parameter estimates with the 95% CI, degrees of freedom (df), F and p values. Mouse ID was included*
503 *as a random effect to take into account the non-independence of observations for the same individual*
504 *over time. N = 94 individuals and 476 observations.*

Fixed effects		**Estimate**	**95% CI**	**df**	**F**	**P**
Treatment				2,373	1.05	0.3518
	non-infected	0				
	single Py	2.1	-1.05/5.25			
	coinfection (groups 4, 5, 6)	1.7	-0.91/4.31			
Time		0.6	-0.54/1.75	1,373	45.87	<0.0001
Squared time		-0.04	-0.18/0.1	1,373	111.07	<0.0001
Cubic time		0.0008	-0.004/0.005		109.01	
Time*Treatment				2,373	17.09	<0.0001
	non-infected	0				
	single Py	-4.36	-5.98/-2.73			
	coinfection (groups 4, 5, 6)	-3.56	-4.92/-2.21			
Squared Time*Treatment				2,373	30.02	<0.0001
	non-infected	0				
	single Py	0.71	0.51/0.90			
	coinfection (groups 4, 5, 6)	0.58	0.41/0.74			
Cubic Time*Treatment				2,373	27.42	<0.0001
	non-infected	0				
	single Py	-0.02	-0.03/0.016			
	coinfection (groups 4, 5, 6)	-0.02	-0.02/0.012			
Random effect		**Estimate**	**SE**	**z**	**p**	
ID		4.28	1.25	3.44	0.0003	

505

506 Given that coinfected hosts had a higher proportion of iRBCs than single infected hosts, a
507 similar rate of renewal of lost RBCs might result in a reduction in tolerance in coinfected mice. We
508 defined tolerance as the slope of the regression of RBC counts on parasitemia, the steeper the slope
509 the weaker the tolerance (i.e., the capacity to cope with the damage induced by the infection). We
510 found that coinfected hosts (groups 4, 5, 6) were less tolerant (i.e., steeper slope) to Py infection
511 compared to single infected mice (table 9; fig. 5f).

512

513

514

515

516 *Table 9. General linear mixed model investigating the relationship between RBC counts (log 10^6/µl) and*

517 *parasitemia (log proportion iRBC) in single Py infected and coinfected (simultaneous infection and Hp*

518 *first) mice. We report the parameter estimates with the 95% CI, degrees of freedom (df), F and p values.*

519 *Mouse ID was included as a random effect to take into account the non-independence of observations*

520 *for the same individual over time. N = 48 individuals and 298 observations.*

Fixed effects		**Estimate**	**95% CI**	**df**	**F**	**P**
Treatment				1,248	8.71	0.0035
	single Py	0				
	Coinfection (groups 4, 5, 6)	-0.199	-0.331/-0.066			
Parasitemia		-0.300	-0.341/-0.259	1,248	646.17	<0.0001
Treatment *Parasitemia				1,248	9.14	0.0028
	single Py	0				
	Coinfection (groups 4, 5, 6)	-0.081	-0.134/-0.028			
Random effect		**Estimate**	**SE**	**z**	**p**	
Mouse ID		0.015	0.006	2.51	0.0061	

521

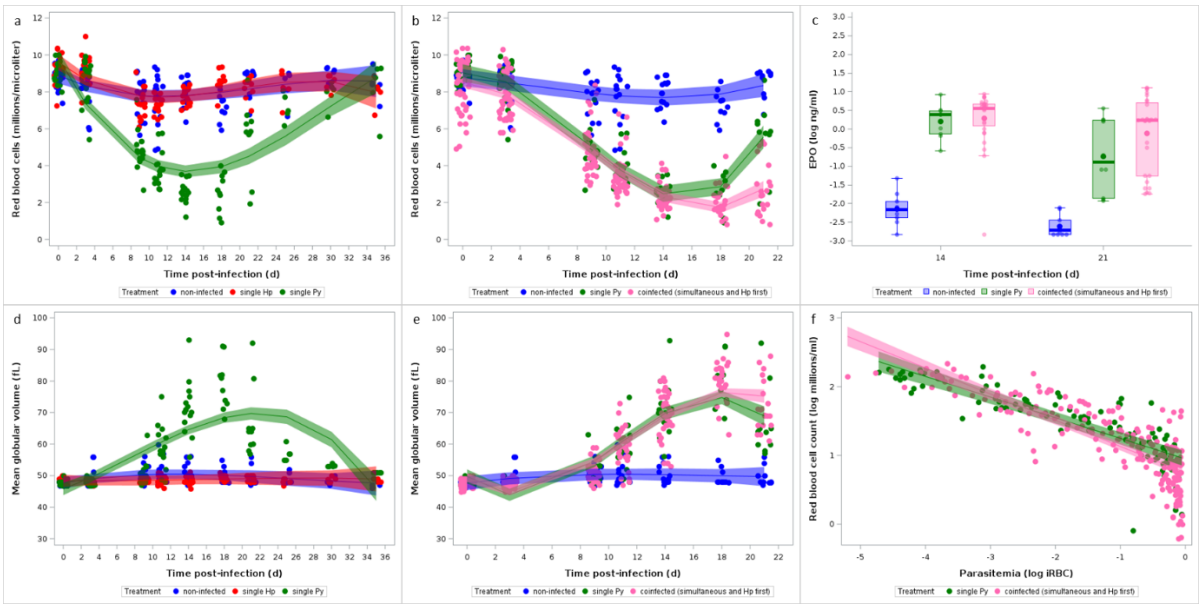

522

523 *Figure 5. Effect of infection and coinfection on RBCs. a) Changes in RBC counts measured by hematology*

524 *analyzer for non-infected and single (Hp, Py) infected mice; b) Changes in RBCs for non-infected, single*

525 *Py infected and coinfected (simultaneous infection and Hp first) groups. Dots represent the raw data,*

526 *the lines represent the fit of the GLMM, and the shaded area around the line the 95% CI. c) Levels of*

527 *erythropoietin (EPO, log ng/ml) in the plasma assessed by ELISA at day 14 and 21 p.i. in non-infected,*

528 *single Py infected and coinfected (simultaneous infection and Hp first) mice. Dots represent the raw*

529 *data, the boxes represent the interquartile range (IQR), the horizontal lines the median, and whiskers*

530 *the range of data within 1.5 the IQR; d) Changes in mean globular volume (MGV, fL) assessed by*

531 *hematology analyzer for non-infected and single (Hp, Py) infected mice; e) Changes in MVG for non-*
532 *infected, single Py infected and coinfected (simultaneous infection and Hp first) groups. Dots represent*
533 *the raw data, the lines represent the fit of the GLMM, and the shaded area around the line the 95% CI;*
534 *f) Log-log plot of RBC counts on parasitemia for single Py infected and coinfected (simultaneous*
535 *infection and Hp first) groups. Dots represent the raw data, the lines represent the fit of the GLMM,*
536 *and the shaded area around the line the 95% CI.*
537
538 If coinfected hosts suffer from more severe disease symptoms because they cannot effectively
539 restore RBCs lost during the infection, we might expect that experimentally inducing erythropoiesis, at
540 least partially, dampen the cost of coinfection. To explore this hypothesis, we ran an experiment where
541 mice were first infected with Hp and after 28 days they were infected with Py. Mice were then treated
542 with a rEPO or left as control. We assessed the severity of the symptoms using an integrative marker
543 of health (body mass), a specific marker of Py infection (changes in RBCs), and any mortality (reaching
544 of the end points) that might have occurred during the course of the infection.
545 Treating coinfected mice with rEPO reduced the severity of the disease symptoms, since body
546 mass remained stable over the course of the infection, while mice in the control group lost body mass
547 from day 14 p.i. onwards (table 10, fig. 6a). rEPO treatment only slightly affected anemia (GLMM, time
548 p.i.*treatment, $F_{1,129} = 4.12$, $p = 0.0443$, n = 20 individuals and 153 observations; fig. 6b, fig. S16), and
549 although mortality was higher in the control group, the difference was not statistically significant (Log-
550 rank test, $\chi^2_1 = 1.059$, $p = 0.3034$, n = 20; fig. 6c), suggesting that other aspects of the pathophysiology
551 of coinfection might explain the observed increase in Py virulence (although it should be acknowledged
552 that larger sample size might have produced a statistically significant difference between groups).
553 Nevertheless, the rEPO administration improved the tolerance to Py infection, since coinfected mice
554 treated with rEPO had similar slope relating RBC counts to parasitemia as single Py infected hosts
555 (GLMM, treatment*parasitemia, $F_{1,111} = 0.11$, $p = 0.7363$, n = 25 individuals and 138 observations; fig.

556 6d). Therefore, coinfection reduced the tolerance to Py infection and administering rEPO partially
557 restored it.
558
559 *Table 10. General linear mixed model investigating the changes in body mass (g) in coinfected (Hp-*
560 *28+Py) mice treated with rEPO or with PBS. We report the parameter estimates with the 95% CI,*
561 *degrees of freedom (df), F and p values. Mouse ID was included as a random effect to take into account*
562 *the non-independence of observations for the same individual over time. N = 20 individuals and 245*
563 *observations.*

Fixed effects		**Estimate**	**95% CI**	**df**	**F**	**P**
Treatment				1,221	0.27	0.6055
	PBS	0				
	rEPO	-0.35	-1.67/0.98			
Time		0.2	0.11/0.29	1,221	31.59	<0.0001
Squared time		-0.012	-0.016/-0.008	1,221	40.36	<0.0001
Time*Treatment				1,221	0.75	0.3878
	PBS	0				
	rEPO	-0.05	-0.18/0.069			
Squared Time*Treatment				1,221	6.78	0.0098
	PBS	0				
	rEPO	0.007	0.002/0.013			
Random effect		**Estimate**	**SE**	**z**	**p**	
ID		1.77	0.61	2.91	0.0018	

564

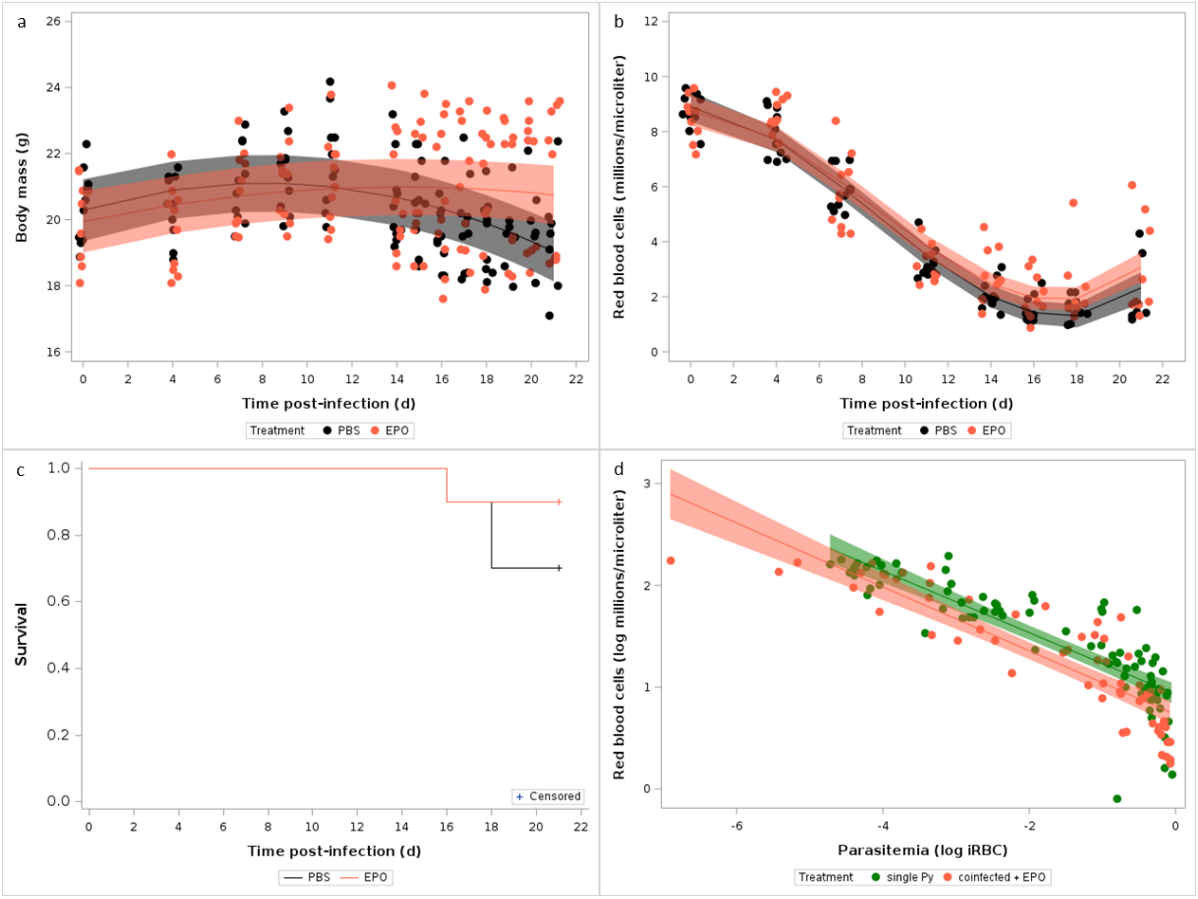

Figure 6. Effect of rEPO administration on the symptoms of the coinfection. a) Changes in body mass (g) over the course of the infection in mice that were infected with Hp at day -28 and with Py at day 0, and treated with rEPO or left as control (PBS); b) Changes in RBC counts assessed by hematology analyzer in coinfected mice treated with EPO or left as control (PBS). Dots represent the raw data, the lines represent the fit of the GLMM, and the shaded area around the line the 95% CI; c) Survival of coinfected mice treated with rEPO or left as control (PBS); d) Log-log plot of RBC counts on parasitemia for single Py infected mice and coinfected (infected with Hp at day -28 and with Py at day 0) mice treated with rEPO. Dots represent the raw data, the lines represent the fit of the GLMM, and the shaded area around the line the 95% CI.

In addition to inducing anemia, the lysis of RBCs releases free heme groups that have pro-oxidant and pro-inflammatory properties, and stimulates the production of enzymes whose role is to scavenge them. We therefore hypothesized that the increased virulence of Py in coinfected hosts (when Py follows Hp) might stem from an impaired capacity to detoxify free heme groups. To this

580 purpose, we assessed the expression of the *Hmox1* gene in splenocytes at day 14 p.i. and the amount
581 of circulating heme oxygenase-1 (HO-1) in plasma at day 14 and 21 post last infection. *Hmox1* was
582 strongly upregulated in Py infected mice compared to non-infected individuals (GLM, $F_{1,8} = 96.92$, n =
583 10; $p < 0.0001$; fig. 7a, fig. S17a), and it was also upregulated in coinfected groups (groups 4, 5, 6)
584 compared to single Py infected hosts (post-hoc comparison of LS-means, p = 0.0074, n = 28; fig. 7a, fig.
585 S17a,b). However, although single Py infected mice also had much higher plasma levels of the enzyme
586 HO-1 at both day 14 and 21 p.i. compared to non-infected individuals (GLM, $F_{1,24} = 82.98$, $p < 0.0001$,
587 n = 28; fig. 7b), coinfected groups (groups 4, 5, 6) did not differ from single Py infection (when
588 considering the different coinfection groups separately, GLM, $F_{3,68} = 2.49$, p = 0.0677, n = 76; fig. S17c;
589 when considering the coinfection groups together, post-hoc comparison of LS-means, p = 1, n = 86; fig.
590 7b). Therefore, although *Hmox1* gene expression was upregulated in the coinfection groups, the level
591 of the enzyme in the blood did not differ between single infection and coinfection.

592 Another important function related to the clearance of free hemoglobin is provided by the
593 scavenger receptor CD163 expressed on red pulp macrophages (RPM, F4/80$^+$ CD11b$^-$) (Kristiansen et
594 al. 2001). We therefore assessed the proportions of RPM that were CD163$^+$, by flow cytometry, and
595 compared them between non-infected and single Py infected and found that the population of CD163$^+$
596 RPM drastically dropped during the infection (generalized linear model with a beta distribution of
597 errors, $F_{1,35} = 344.88$, $p < 0.0001$, n = 39; fig. 7c). However, the proportion of RPM that were CD163$^+$
598 was similarly reduced in coinfected mice (groups 4, 5, 6) compared to single Py infection, at both day
599 14 and 21 p.i. (LS-means comparison with Bonferroni correction, day 14 p.i., p = 0.1648, day 21 p.i., p
600 = 0.1959, n = 100; fig. 7c, fig. S17d). The receptor CD163 was also less expressed in F4/80$^+$ CD11b$^-$ of
601 Py infected mice, as shown by the drastic drop in mean fluorescence intensity (MFI), with no difference
602 between single and coinfected mice (LS-means comparison with Bonferroni correction, day 14 p.i., p =
603 1, day 21 p.i., p = 1, n = 100; fig. 7d). Therefore, the population of CD163$^+$ RPM which are a key resident
604 cell population responsible for clearing free hemoglobin released during the lysis of RBCs similarly
605 decreased in single and coinfected mice.

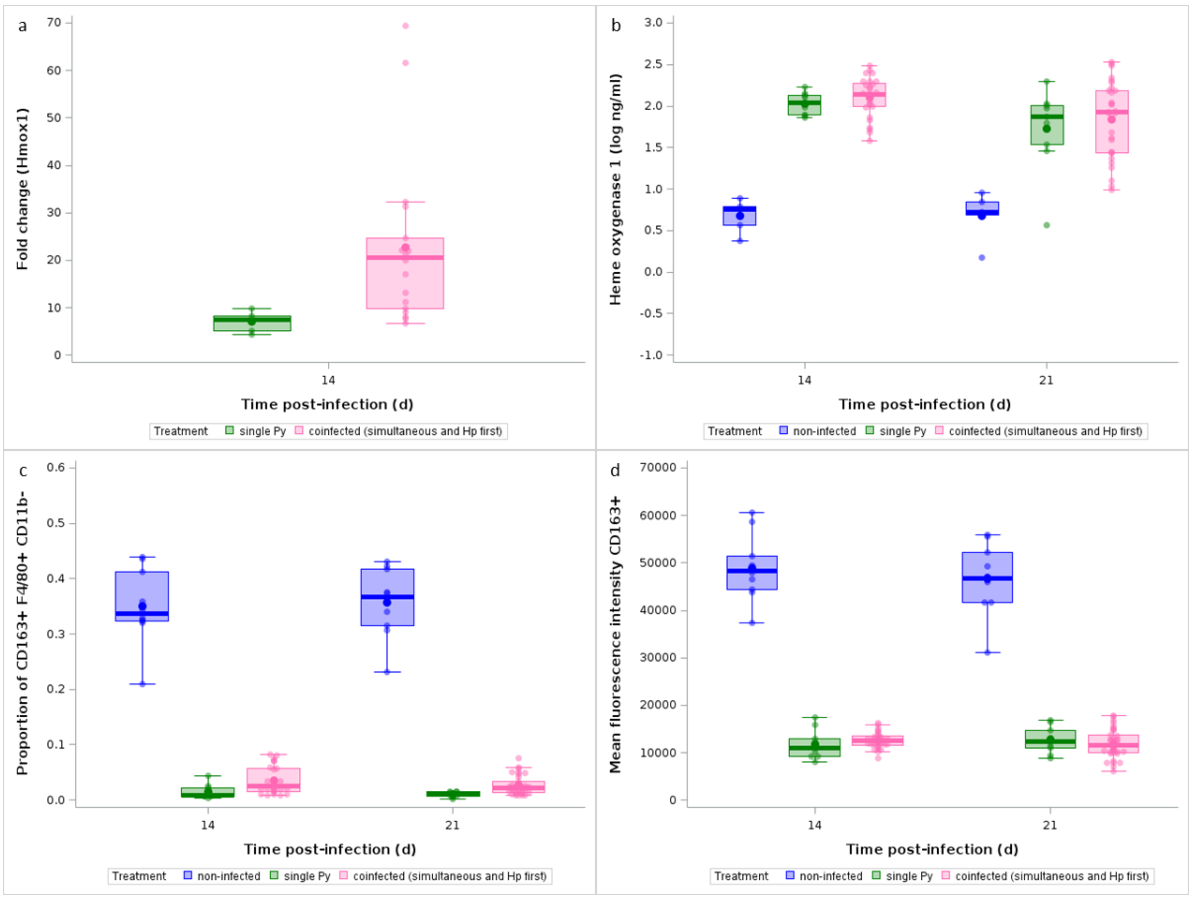

Figure 7. Effect of infection and coinfection on heme detoxification. a) Fold change relative to non-infected mice of Hmox1 mRNA in spleen at day 14 p.i. in single Py infected and coinfected (simultaneous infection and Hp first) groups; b) Levels of Heme oxygenase-1 in the plasma (log ng/ml) at day 14 and 21 p.i. in non-infected, single Py infected and coinfected (simultaneous infection and Hp first) groups; c) Proportion of CD163^{+} within F4/80^{+} CD11b^{-} cells analyzed by flow cytometry at day 14 and 21 p.i. in non-infected, single Py infected and coinfected (simultaneous infection and Hp first) groups; d) Mean fluorescence intensity (arbitrary fluorescence units) of CD163 at day 14 and 21 p.i. in non-infected, single Py infected and coinfected (simultaneous infection and Hp first) groups. Dots represent the raw data, the boxes represent the interquartile range (IQR), the horizontal lines the median, and whiskers the range of data within 1.5 the IQR.

Immune predictors of Py virulence

Plasmodium infection elicits proinflammatory effectors that might cause immunopathology if regulatory mechanisms fail to restore homeostasis. Therefore, we speculated that exacerbated disease

severity in coinfected hosts (when Py follows Hp) might stem from an overreacting, non-regulated, inflammatory response. To address this question, we first assessed the gene expression of pro- (IFN-γ) and anti-inflammatory (IL-10, TGF-β) cytokines in splenocytes at day 3 and 14 post-infection. IFN-γ, IL-10 and TGF-β1 genes were all overexpressed at both 3 and 14 days p.i. in single Py infected hosts compared to non-infected mice (GLM, IFN-γ, $F_{1,34} = 24.44$, $p < 0.001$; IL-10, $F_{1,34} = 49.86$, $p < 0.001$; TGF-β, $F_{1,34} = 20.62$, $p < 0.001$, n = 38; fig. 8; fig. S18a,b,c). However, coinfection (groups 4, 5, 6) did not induce a change in the expression of any of the genes compared to single Py infection (LS-means comparison with Bonferroni correction, all p's = 1, fig. 8, fig. S18d,e,f).

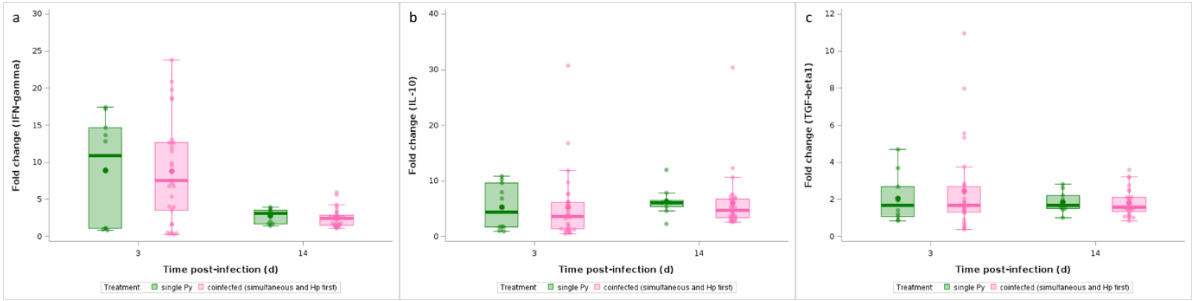

Figure 8. Effect of infection and coinfection on cytokine expression. Fold change (relative to non-infected hosts) of a) IFN-γ, b) IL-10, c) TGF-β1 mRNA levels in spleen at day 3 and 14 p.i. in single Py infected and coinfected (simultaneous infection and Hp first) groups. Dots represent the raw data, the boxes represent the interquartile range (IQR), the horizontal lines the median, and whiskers the range of data within 1.5 the IQR.

Previous work conducted on the same model system has shown that coinfected mice have a higher activation of regulatory T cells (Treg), possibly accounting for their impaired anti-*Plasmodium* response (Tetsutani et al. 2009). Therefore, we assessed the proportions of $CD4^+$ T cells that were $FoxP3^+$ by flow cytometry and compared them, over the course of the infection, between non-infected, single Py infected and coinfected mice (groups 4, 5, 6); we found no differences between single Py infection and coinfection groups (LS-means comparison with Bonferroni correction, p = 1; n = 100; fig. 9a, table S15; fig. S19a). The expression of the immune checkpoint CTLA-4 on Treg has been shown to impede immunity to the acute infection with Py (Kurup et al. 2017), by enhancing their

644 immunosuppressive activity. We thus assessed the proportions of CD4⁺ T cells that were FoxP3⁺ and
645 CTLA-4⁺ by flow cytometry and compared them between non-infected, single Py infected and
646 coinfected mice (groups 4, 5, 6); we found that coinfected mice had a higher proportion of CTLA-4⁺
647 Treg compared to non-infected and single Py infection at day 14 p.i. (table 11; fig. 9b; table S16; fig.
648 S19b). Therefore, although coinfection did not produce an expansion of the Treg population compared
649 to single Py infected hosts, the immunosuppressive power of Treg was upregulated in coinfected hosts.
650

651 *Table 11. Generalized linear model with a beta distribution of errors investigating the changes in the*
652 *proportion of CTLA-4⁺ within FoxP3⁺ CD4⁺ T cells in non-infected, single Py infected and coinfected*
653 *(simultaneous infection and Hp first) mice at day 14 and 21 post-infection. We report the degrees of*
654 *freedom (df), and the F and p values. N = 96 individuals.*

Source of variation	df	F	P
Treatment	2,90	19.01	<0.0001
Time	1,90	0.79	0.3755
Time*Treatment	2,90	13.89	<0.0001

655

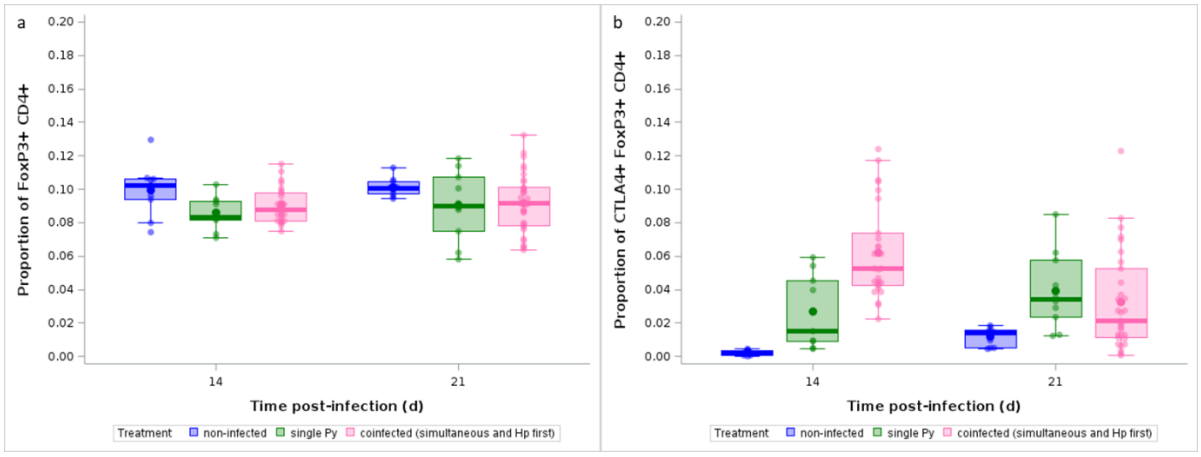

656
657 *Figure 9. Effect of infection and coinfection on Treg expansion and immunosuppressive function. a)*
658 *Proportion of FoxP3⁺ within CD4⁺ T cells analyzed by flow cytometry over the course of the infection in*
659 *non-infected, single Py infected and coinfected (simultaneous infection and Hp first) mice; b) Proportion*
660 *of CTLA-4⁺ within FoxP3⁺ CD4⁺ T cells analyzed by flow cytometry over the course of the infection in*
661 *non-infected, single Py infected and coinfected (simultaneous infection and Hp first) mice. Dots*

662 *represent the raw data, the boxes represent the interquartile range (IQR), the horizontal lines the*
663 *median, and whiskers the range of data within 1.5 the IQR.*
664
665 Using flow cytometry, we also immunophenotyped mice using a large panel of markers in the
666 spleen (table S2), at day 3, 14 and 21 post last infection. We identified 20 cell populations (table S17)
667 and their proportions were included as variables in a principal component analysis (PCA), with a PCA
668 per sampling day. The first two components explained 29.02% and 18.79%, 39.65% and 12.86%,
669 37.63% and 15.92% of the total variance, at day 3, 14, and 21 p.i., respectively. The correlation circles
670 showed that many of the variables included in the PCA had high absolute loadings (table S17, fig. S20a,
671 b, c). At day 3 p.i., the scores along the first principal component (PC1) strongly differed between the
672 three experimental groups (GLM, $F_{2,45} = 28.56$, n = 48; $p < 0.0001$), with coinfected mice (groups 4, 5,
673 6) having higher scores compared to both non-infected and single Py infection (LS-means comparisons
674 with Bonferroni correction, both p's < 0.0001; fig. S20d). At day 14 and 21 p.i., there was a complete
675 separation, along the PC1, between the three groups, with single Py infected lying in between non-
676 infected and coinfected individuals (groups 4, 5, 6) (day 14 p.i.: GLM, $F_{2,43} = 313.37$, $p < 0.0001$, n = 46;
677 day 21 p.i.: GLM, $F_{2,51} = 257.50$, $p < 0.0001$, n = 54; fig. S20d). The PC2 had a much less discriminant
678 power among groups (day 3 p.i.: GLM, $F_{2,45} = 3.02$, p = 0.0588, n = 48; day 14 p.i.: GLM, $F_{2,43} = 1.27$, p =
679 0.2902, n = 46; day 21 p.i.: GLM, $F_{2,51} = 7.57$, p = 0.0013, n = 54; fig. S20e).
680 To go further, we focused on the variables that had strong absolute loadings on the PC1 and
681 compared them between the groups, with the aim to see if there was a consistent difference between
682 single Py infected and coinfected hosts (groups 4, 5, 6). The proportion of Th2 (proportion of $CD4^+$ T
683 cells that were GATA-3^+) differed between single and coinfected hosts at the three sampling dates
684 (GLM with a beta distribution of errors, $F_{2,139} = 53.91$, $p < 0.0001$, n = 148; LS-means comparison
685 between single and coinfected with Bonferroni correction, day 3, p = 0.0002; day 14, p = 0.0102; day
686 21, $p < 0.0001$; fig. 10a). Among the other variables, only $CD8^+$ T cells consistently discriminated
687 between single Py and coinfected hosts (groups 4, 5, 6), with the proportion of $CD8^+$ T cells (proportion

688 of CD3$^+$ that were CD8$^+$) sharply decreasing over time and especially so in coinfected hosts (GLM with
689 a beta distribution of errors, $F_{2,139} = 347.41$, $p < 0.0001$, n = 148; LS-means comparison between single
690 and coinfected with Bonferroni correction, day 3, p = 1; day 14, $p < 0.0001$; day 21, $p < 0.0001$, fig.
691 10b).

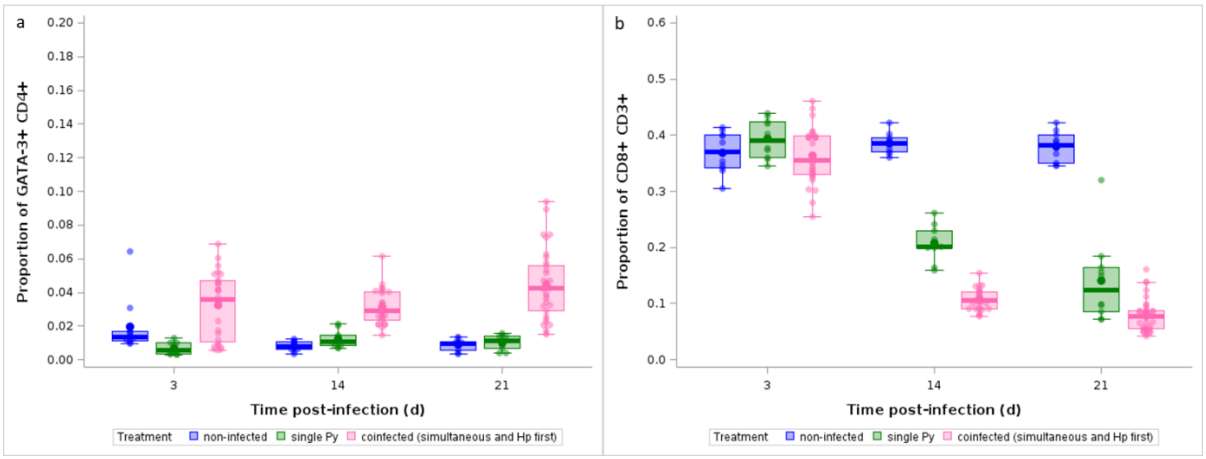

692
693 *Figure 10. Effect of infection and coinfection on Th2 and CD8$^+$ T cells. a) Proportion of GATA-3$^+$ within*
694 *CD4$^+$ T cells and b) proportion of CD8$^+$ within CD3$^+$ T cells analyzed by flow cytometry over the course*
695 *of the infection in non-infected, single Py infected and coinfected (simultaneous infection and Hp first)*
696 *hosts. Dots represent the raw data, the boxes represent the interquartile range (IQR), the horizontal*
697 *lines the median, and whiskers the range of data within 1.5 the IQR.*

698

699 Therefore, Th2 and CD8$^+$ T cells were the two populations that best discriminated between Py
700 infected and coinfected hosts (when Py follows Hp). While the effect of coinfection on the rise of Th2
701 lymphocytes can easily be understood as the direct consequence of Hp induction of Th2 immunity, we
702 wished to better investigate the reasons underlying the decrease of CD8$^+$ T cells in coinfected mice. To
703 this purpose, we assessed the proportion of CD8$^+$ T cells that expressed three immune checkpoints in
704 non-infected, single Py infected and coinfected hosts (groups 4, 5 and 6), and predicted that coinfected
705 mice should have higher proportions of CD8$^+$ T cells expressing the immune checkpoints compared to
706 single Py infection. Py infection enhanced the proportion of CTLA-4$^+$ CD8$^+$ T cells (proportion of CD8$^+$
707 that were CTLA-4$^+$) but there was no difference between single infection and coinfection (groups 4, 5
708 and 6) at any of the sampling day (GLM with a beta distribution of errors: day 14 p.i, t = -0.52, df = 90,

709 p = 1; day 21 p.i., t = -1.19, df = 90, p = 1; fig. 11a). The proportions of LAG-3$^+$ CD8$^+$ and PD-1$^+$ CD8$^+$ cells

710 (proportion of CD8$^+$ that were LAG-3$^+$ and PD-1$^+$, respectively) were also increased in infected mice

711 compared to non-infected individuals, however, at day 14 p.i. there was also a higher proportion of

712 LAG-3$^+$ and PD-1$^+$ CD8$^+$ T cells in coinfected mice compared to single Py infection (GLM with a beta

713 distribution of errors: LAG-3, day 14 p.i.: t = 3.38, df = 91, p = 0.0163; day 21 p.i., t = 2.36, df = 91, p =

714 0.3040; PD-1, day 14 p.i.: t = 3.94, df = 90, p = 0.0024; day 21 p.i., t = 2.26, df = 91, p = 0.3948, fig.

715 11b,c).

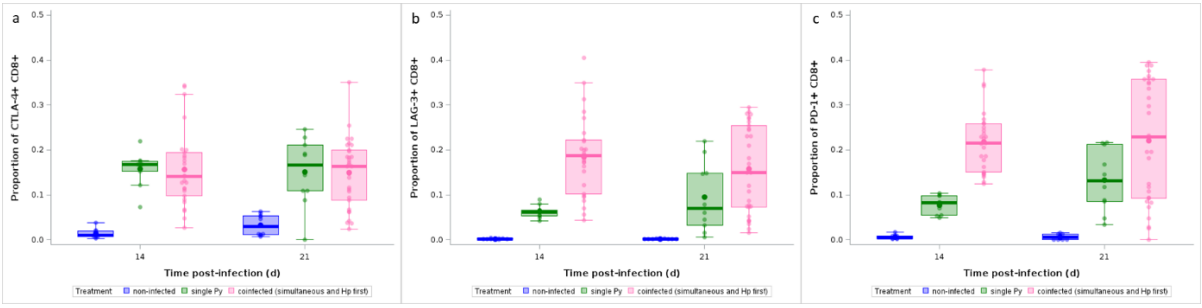

716

717 *Figure 11. Effect of infection and coinfection on CD8$^+$ T cell exhaustion. a) Proportion of CTLA-4$^+$ within*

718 *CD8$^+$ T cells, b) LAG-3$^+$ within CD8$^+$ T cells, c) PD-1$^+$ within CD8$^+$ T cells analyzed by flow cytometry at day*

719 *14 and 21 p.i. in non-infected, single Py infected and coinfected (simultaneous infection and Hp first)*

720 *hosts. Dots represent the raw data, the boxes represent the interquartile range (IQR), the horizontal*

721 *lines the median, and whiskers the range of data within 1.5 the IQR.*

722

723 Persistent antigenic stimulation and high levels of inhibitory receptors (immune checkpoints)

724 can lead to the exhaustion of CD8$^+$ T cells, characterized by a loss of effector functions and proliferative

725 potential (McLane et al. 2019), and to the increase in the CD4$^+$/CD8$^+$ ratio above the homeostatic value

726 (between 1.5 and 2.5) (McBride and Striker 2017). Deviations from this homeostatic value have been

727 associated with severe symptoms in a few infectious diseases (e.g., Pascual-Dapena et al. 2022). We

728 therefore wished to investigate if high values of the CD4$^+$/CD8$^+$ ratio also predicted mortality in our

729 system. We could not investigate this point at the individual level because data on the proportion of

730 immune cells were gathered on mice that were euthanized at specific days post last infection.

731 Nevertheless, we could correlate the CD4$^+$/CD8$^+$ ratio at day 14 and 21 p.i. with the mortality rate (the

732 proportion of mice reaching the end points) within each experimental group and found that indeed
733 the higher the ratio the higher the mortality risk (spearman correlation, Rs = 0.766, n = 100, p < 0.0001,
734 fig. 12).

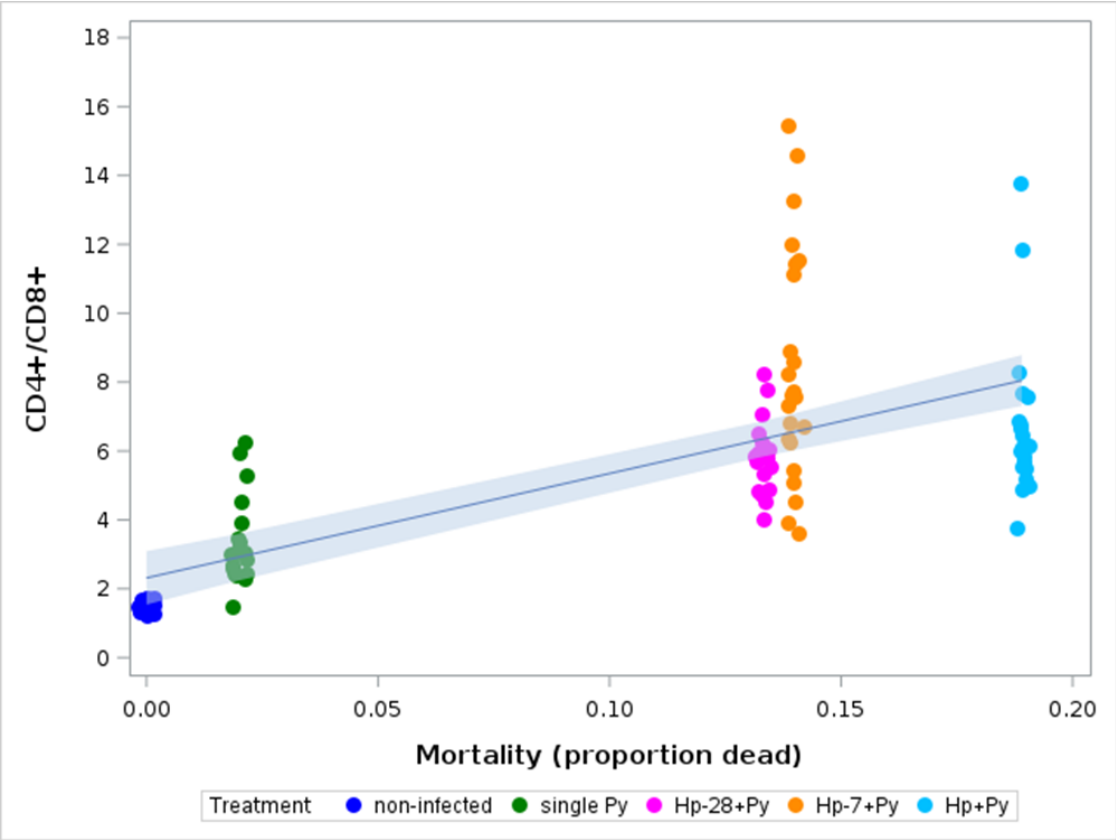

735
736 *Figure 12. Correlation between the CD4⁺/CD8⁺ ratio at day 14 and 21 p.i. and the mortality rate in non-*
737 *infected, single Py infected and coinfected (simultaneous infection and Hp first) hosts. Mortality refers*
738 *to the proportion of hosts reaching the experimental end points within groups. Dots represent the raw*
739 *data, the line represents a linear regression fit and the band the 95% CI of the slope.*

740

741 **Discussion**

742 We showed that the order of infection plays a paramount role in determining the outcome of
743 the coinfection between an intestinal nematode and a *Plasmodium* parasite. In particular, Py virulence
744 increased when infecting hosts that were previously or simultaneously infected with Hp, compared
745 both to hosts with single infections and to hosts that were infected with Py first and then with Hp.
746 Contrary to Py, virulence of Hp was minimally affected by the coinfection. These results are partially in

747 agreement with our initial predictions. We hypothesized that previous infection with either Py or Hp
748 would polarize the immune response towards Th1 or Th2 effectors making hosts more susceptible to
749 a subsequent infection. This prediction was met when Py infected mice harboring Hp, but not when
750 Hp infected mice harboring Py. Therefore, there is a strong asymmetry in the effect of coinfection
751 between Py and Hp, depending on the order of the infection. The increase in Py virulence in mice
752 previously infected with Hp is consistent with previous results on this system (Tetsutani et al. 2009),
753 suggesting that previous Hp infection impairs the subsequent immune response to Py (Noland et al.
754 2008; Tetsutani et al. 2009).

755 The possible evolutionary reasons underlying this asymmetry are manifold. Intestinal
756 nematodes usually produce chronic infections where the hosts keep shedding parasite eggs for months
757 or even years depending on the species (Morand 1996). Inter-host transmission success and parasite
758 fitness is tightly associated with the duration of egg shedding (patent period), therefore any parasite
759 trait that compromises host health and survival is likely counter selected in these systems. In
760 agreement with this view, nematode infections are usually well tolerated and host damage is usually
761 observed only when parasite burden is high (Brooker 2010; Lippens et al. 2016). Since reinfection was
762 not possible in our experiment, parasite burden was constrained by the initial number of infective
763 larvae given to the host. It might be interesting to investigate to what extent the lack of increase in Hp
764 virulence in coinfected hosts could change when using higher infective doses (Lippens et al. 2016), or
765 allowing hosts to be reinfected. Although the transmission success of Py cannot be directly assessed
766 from the proportion of iRBC, longer persistence of high parasite density, as observed in coinfected
767 hosts, should increase the likelihood of gametocyte production, as reported for other *Plasmodium*
768 species (see Tadesse et al. 2017). In agreement with this view, Py transmission success to the dipteran
769 vector was enhanced when mice were coinfected with the helminth *Echinostoma caproni* (Noland et
770 al. 2007). Therefore, the cost of virulence is probably higher in Hp than in Py. Alternatively, increased
771 Py virulence might be maladaptive if host overexploitation and death jeopardize parasite fitness
772 through reduced transmission success.

773 Whatever the benefit or disadvantage of changes in virulence for Py, from the host
774 perspective, coinfection did incur costs both in terms of general health and specific markers of Py
775 infection. In particular, while single infected hosts still gained mass during the 5 weeks p.i., at a rate
776 that was similar to the non-infected hosts, coinfection induced a loss of body mass (simultaneous
777 infection and when Py infected mice previously infected with Hp) or temporarily slowed down the gain
778 in body mass (when Hp infected mice previously infected with Py). In agreement with the results on
779 changes in body mass, host mortality (reaching of the end points) was only reported in coinfection
780 groups where Py followed the Hp infection (and the simultaneous infection). Interestingly, there was
781 no difference according to the timing of the infection, suggesting that the importance of the order of
782 the infection is conserved and relatively consistent over different coinfection scenarios. In another
783 coinfection model, involving the cestode *Taenia crassiceps* and *Plasmodium yoelii* 17XL, Salazar-
784 Castañón et al. (2018) found that coinfected mice had relatively longer survival time compared to
785 single Py infected hosts and that the gain in survival was related to the timing of the infection (the
786 longer the delay between the infection, the better the gain in survival time), suggesting that the effect
787 of timing of infection might be model-dependent.

788 Our prediction of increased virulence in coinfected hosts was based on the rationale that
789 previous infection with nematodes polarizes the immune system towards a Th2 response (Reynolds et
790 al. 2012). In agreement with this hypothesis, we found that Th2 cells discriminated the three
791 experimental groups, with higher percentage of GATA-3^{+} within CD4^{+} T cells in coinfected hosts (when
792 Py follows Hp) compared to both single Py infected and non-infected mice. Accordingly, we also
793 predicted that coinfected mice should have an impaired capacity to deal with Py infection and indeed
794 we found that parasitemia was still high at day 21 p.i. in coinfected hosts compared to single Py
795 infected mice. Therefore, direct damage produced by Py multiplication might account for the more
796 severe disease symptoms observed in coinfected hosts. In agreement with this view, changes in RBC
797 counts over the course of the infection mirrored changes in parasitemia, with coinfected groups still
798 suffering from anemia at day 21 p.i., when single Py infected mice had already started to recover.

799 The fitness consequences of the damage caused by Py multiplication also depend on the host
800 capacity to repair damaged tissues, or in other terms on the capacity to tolerate the infection
801 (Medzhitov et al. 2012). In particular, RBCs are constantly renewed during hematopoiesis and
802 therefore hosts that can restore lost RBCs at a faster pace should be able to better tolerate the
803 infection (i.e., to pay a smaller infection cost) compared to hosts with a slower rate of RBC renewal
804 (Chang et al. 2004). Given that coinfected hosts suffered from higher anemia, compensating for the
805 higher rate of RBC loss would have needed a higher production of reticulocytes. However, we found
806 that coinfected hosts had similar plasma levels of EPO and similar proportions of reticulocytes, as
807 assessed by the MGV, compared to single infected hosts. Therefore, despite higher parasitemia and
808 higher anemia, coinfected hosts only replaced RBCs at a similar rate of single infected hosts. This
809 finding suggests that any improvement of the capacity to renew lost RBCs should reduce the cost of
810 coinfection. Experimental administration of rEPO to coinfected hosts partially improved the symptoms
811 of the disease, as also previously reported (Kaiser et al. 2006), and improved host tolerance to the
812 infection. However, the magnitude of the effects was small, suggesting that other aspects of the
813 physiopathology of the coinfection might be important determinants of the coinfection costs.
814 Moreover, there are physiological constraints that set a limit to the maximum daily rate of RBC
815 production, including the number of hematopoietic stem cells that can be committed to become
816 reticulocytes or the saturation of EPO receptors (Suzuki et al. 2002, Comazzetto et al. 2019). In
817 addition, the production of reticulocytes also replenishes the reservoir of cells that can be exploited
818 by Py for its own replication, which can also contribute to maintain parasitemia over longer period of
819 time and possibly exacerbates disease severity (Chang et al. 2004; Tsubata et al. 2005).

820 Massive release of free heme groups has the potential to damage host tissues through their
821 prooxidant, proinflammatory and cytotoxic effects (Kumar and Bandyopadhyay 2005; Immenschuh et
822 al. 2017). Previous studies have shown that the effectiveness of the mechanisms of detoxification of
823 free heme groups are key determinants of host survival (Pamplona et al. 2007; Seixas et al. 2009) and
824 liver function restoring once the parasite has been cleared (Dey et al. 2014), although the anti-

825 inflammatory properties of HO-1 might also promote liver infection (Epiphanio et al. 2008). We
826 therefore assessed the expression of the *Hmox1* gene in splenocytes and the amount of the enzyme
827 HO-1 in plasma. As for the renewal of lost RBCs, given that coinfected hosts had higher amount of free
828 hemoglobin compared to single infection (due to the higher RBC lysis), we expected to find a higher
829 expression of *Hmox1* and more HO-1 in plasma of coinfected hosts. However, although the gene was
830 overexpressed in coinfected mice (the gene was highly overexpressed in infected mice compared to
831 non-infected hosts), the amount of enzyme was similar in coinfected and single Py infected hosts,
832 possibly due to the degradation of the enzyme through the ubiquitin-proteasome system (Lin et al.
833 2008; Chau 2015). We also found that another mechanism allowing the host to deal with free
834 hemoglobin (the scavenger receptor CD163) (Kristiansen et al. 2001) was downregulated in RPM of
835 coinfected and single infected hosts.

836 Free heme group is also recognized as a DAMP by the immune system and can induce an
837 overreacting inflammatory response leading to host damage (Fortes et al. 2012). Coinfection between
838 Hp and another model species of murine malaria (*Plasmodium chabaudi* AS) has been reported to
839 increase host mortality (Su et al. 2005), due to liver pathology involving hepatic IFN-γ, IL-17 and IL-22
840 (Helmby 2009). Although infected hosts overexpressed IFN-γ, IL-10 and TGF-β1 compared to non-
841 infected mice, there was no difference between coinfected and single Py infected mice. Similarly, we
842 did not find any difference in the percentage of $FoxP3^+$ within $CD4^+$ T cells between single Py infected
843 and coinfected mice; however, the percentage of CTLA-4^+ within $FoxP3^+$ $CD4^+$ T cells was higher in
844 coinfected mice compared to single Py infected hosts during the peak of the acute infection. Therefore,
845 although we did not find an expansion of Treg in Py infected mice (as previously shown, Tetsutani et
846 al. 2009), the immunosuppressive capacities of Treg were upregulated in single Py infected mice, and
847 even more so in coinfected hosts through the CTLA-4 immune checkpoint (see Kurup et al. 2017).
848 Therefore, coinfected mice appeared to have an upregulated immunosuppressive function, possibly
849 accounting for the failure to control Py multiplication.

850 We went a step further by identifying 20 immune cell populations in the spleen by spectral
851 flow cytometry using a 27-color panel. The results of the PCA clearly showed that the three
852 experimental groups clustered in different areas of the space defined by the first two components,
853 and especially so at day 14 and 21 p.i., with the single Py infection group lying in between the non-
854 infected and the coinfection groups. The cell population that best discriminated between single Py
855 infected and coinfected hosts was the $CD8^+$ T cells that got exhausted more in coinfected mice. Several
856 Py epitopes are recognized by $CD8^+$ T cells during the blood stage of the infection (Howland et al. 2015).
857 Moreover, previous work has shown that $CD8^+$ T cells play a role in the protective immunity against
858 blood-stage infection with Py (Imai et al. 2010), and chronic infection with the nematode *Litosomoides*
859 *sigmodontis* interferes with the anti-*Plasmodium* $CD8^+$ T cell response (Kolbaum et al. 2012). Infection
860 with Hp has also been shown to suppress $CD8^+$ T cells in mice subsequently infected with the protozoan
861 *Toxoplasma gondii* (Khan et al. 2008). Exhaustion of $CD8^+$ cells results from the overexpression of
862 immune checkpoints whose function is to avoid immunopathology during persistent antigenic
863 exposure (Chandele et al. 2010; Wykes and Lewin 2018; McLane et al. 2019). In agreement with this,
864 we found that the proportion of both PD-1^+ and LAG-3^+ within $CD8^+$ T cells was higher in coinfected
865 hosts compared to single Py infection at day 14 post last infection. Mechanisms supposed to protect
866 the hosts from immunopathology (Howland et al. 2015) might thus actually make them more
867 susceptible to parasite exploitation (Scholzen et al. 2009; Frimpong et al. 2019), and especially so when
868 hosts are coinfected by parasites with different exploitation strategies.
869 One of the consequences of the $CD8^+$ exhaustion is an increase of the ratio between $CD4^+$ and
870 $CD8^+$ T cells. Deviations of the $CD4^+/CD8^+$ ratio from the homeostatic values (inverted ratio below 1, or
871 increased values above 2.5) have been investigated in a few host-pathogen systems, and found to
872 correlate with poor host survival prospects (McBride and Striker 2017). For instance, high values of the
873 $CD4^+/CD8^+$ ratio have been shown to be predictors of patient mortality during SARS-CoV-2 infection
874 (De Zunai et al. 2021; Pascual-Dapena et al. 2022). We found similar results, although the correlation
875 between the $CD4^+/CD8^+$ ratio and mortality could only be assessed at the population (inter-group)

876 level. The increase of the $CD4^+/CD8^+$ ratio probably reflects a global, temporary, dysfunction of the
877 immune response, which favors the replication rate of Py in coinfected hosts. In agreement with this
878 view, BALB/c mice infected with Py and depleted of $CD8^+$ T cells suffered from greater parasitemia and
879 higher mortality compared to control individuals during the period of peak parasitemia (Imai et al.
880 2015).

881 This work provides some relevant findings for the epidemiology of the coinfection between
882 nematodes and *Plasmodium* and possibly for the evolution of virulence when parasites exploit the
883 same host. In terms of the epidemiology of the disease, a key question is whether infection order is
884 random or if it intrinsically depends on the life cycle of the parasite. In the specific case of the
885 coinfection between gastrointestinal nematodes and *Plasmodium*, hosts might have higher chances to
886 suffer from ordered infections where *Plasmodium* infects hosts already harboring worms. This
887 suggestion is based on the observation that gastrointestinal nematodes usually establish chronic,
888 steady state, infections that can last for months (or even years for some human helminths) while
889 *Plasmodium* produces acute infections (lasting 2-4 weeks) that can either be cleared or lead to
890 subsequent relapses (again depending on the parasite and the host species). However, this hypothesis
891 rests on the assumption that hosts have equal probabilities to be infected by the two parasites per unit
892 of time, or in other words that the probability of infection is not age-dependent. Actually, age-
893 dependent infection might depend on the local epidemiological conditions. In areas of malaria
894 hyperendemicity (high transmission rate and high R_0), it is plausible that children are first infected with
895 *Plasmodium* (Natama et al. 2018, Buchwald et al. 2019, Trape et al. 2024) and only at later ages by
896 gastrointestinal nematodes. However, this pattern is likely to change in areas of low malaria
897 transmission (low R_0) where children might acquire helminth infection first (Blouin et al. 2018, Chis
898 Ster et al. 2021), and still harbor them in case of subsequent *Plasmodium* infection. It should also be
899 reminded that our experimental work only considered primary infections (reinfection was not
900 allowed). However, in the real world, hosts are repeatedly exposed to multiple parasites and when
901 there is no sterilizing immunity, previous infection does not fully prevent subsequent reinfection. The

902 complexity due to age-dependent probability of infection and repeated exposure/infection might
903 therefore blur the importance of the infection order as a driver of disease severity in natural settings.
904 Our results also suggest that the campaigns of deworming that have been implemented in
905 several countries with the aim of reducing the negative effects of helminthiases on infant physical and
906 cognitive development, might also have indirect benefits in terms of reduced severity of malaria
907 symptoms, although the epidemiological surveys that have been published so far have reported been
908 inconclusive results (Afolabi et al. 2021, Dila et al. 2022). However, we should keep in mind that
909 interacting organisms exert reciprocal selection pressures and any prediction on the effect of
910 deworming should also consider the microevolutionary response of the coinfecting pathogen. With
911 this respect, our results might also be relevant to predict how selection might shape the optimal level
912 of virulence (defined as infection-induced host damage) when parasites exploit hosts that harbor
913 coinfecting parasites that elicit different immune effectors. A key prediction here is that species-
914 specific cost of virulence might constraint the evolution of host damage in different ways in coinfecting
915 parasites, and shape the optimal strategy of immunomodulation in species that rely on host immune
916 suppression for long-term persistence. Experimental evolution and theoretical modelling would be
917 valuable tools to explore these questions. A final thought is that, although we considered that the
918 coinfection dynamics with *Plasmodium* and nematodes is regulated by top-down mechanisms
919 involving the host immune response, we cannot ignore that both parasites (and nematodes in
920 particular) can also interfere with the host immune response for their own benefit. This paves the way
921 for a scenario where the top-down mechanisms might also be under parasite control.

922 **Conclusion**

923 To conclude, our integrative approach provided several lines of evidence showing that the
924 order of infection is an important factor shaping the severity of disease symptoms in
925 nematode/malaria coinfected hosts. From a more mechanistic perspective, our results suggest that
926 this order-dependent disease severity stems from the trade-off between specific immune effectors
927 that provide protection against either nematodes or *Plasmodium*. We hope that these results will

928 stimulate further research on both the importance of infection order under natural settings, and the
929 potential epidemiological, and public health consequences of large-scale helminth removal through
930 deworming campaigns.
931
932 **Acknowledgments**
933 We are grateful to Valérie Saint Giorgio and all the staff of the animal facility for taking care of the
934 animals.
935 **Funding**
936 The work has been funded by the French Agence Nationale de la Recherche (grant # ANR-21-CE35-
937 0015).
938 **Author contribution**
939 GS, BF, MR and BR conceived the study and gathered the funding; AD, LB, NP, GS and BF collected the
940 data; AD, LB, EG performed the lab work; NP assisted with the spectral flow cytometry analysis; GS
941 analyzed the data; GS, AD and LB wrote the first draft of the manuscript; all authors revised and
942 approved the final version.
943 **Data availability statement**
944 All the data and codes are available in DRYAD (DOI: 10.5061/dryad.0gb5mkmcb).
945 **Conflict of interest**
946 The authors declare no conflict of interest.
947
948 **References**
949 Adegnika AA, Kremsner PG. 2012. Epidemiology of malaria and helminth interaction: e review from
950 2001 to 2011. Current Opinion in HIV and AIDS 7: 221-224.
951 Afolabi MO, Ale BM, Dabira ED, Agbla SC, Bustinduy AL, Ndiaye JLA, Greenwood B. 2021. Malaria and
952 helminth co-infections in children living in endemic countries: A systematic review with meta-
953 analysis. PLoS Neglected Tropical Diseases 15: e0009138.

954 Alizon S, de Roode JC, Michalakis Y. 2013. Multiple infections and the evolution of virulence. Ecology
955 Letters 16, 556-567.
956 Bansemir AD, Sukhdeo MVK. 1994. The food resource of adult *Heligmosomoides polygyrus* in the small
957 intestine. Journal of Parasitology 80, 24.
958 Billet LS, Wuerthner VP, Hua J, Relyea RA, Hoverman JT. 2020. Timing and order of exposure to two
959 echinostome species affect patterns of infection in larval amphibians. Parasitology 147: 1515-
960 1523.
961 Blouin B, Casapia M, Joseph L, Gyorkos TW. 2018. A longitudinal cohort study of soil-transmitted
962 helminth infections during the second year of life and associations with reduced long-term
963 cognitive and verbal abilities. PLoS Neglected Tropical Diseases 12: e0006688.
964 Brooker S. 2010. Estimating the global distribution and disease burden of intestinal nematode
965 infections: Adding up the numbers – A review. International Journal for Parasitology 40: 1137-
966 1144.
967 Buchwald AG, Sorkin JD, Sixpence A, Chimenya M, Damson M, Wilson ML, Seydel K, Hochman S,
968 Mathanga D, Taylor TE, Laufer MK. 2019. Association between age and *Plasmodium falciparum*
969 infection dynamics. American Journal of Epidemiology 188: 169-176.
970 Budischak SA, Wiria AE, Hamid F, Wammes LJ, Kaisar MMM, van Lieshout L, Sartono E, Supali T,
971 Yazdanbakhsh M, Graham AL. 2018. Competing for blood: the ecology of parasite resource
972 competition in human malaria-helminth co-infections. Ecology Letters 21: 536.
973 Chandele A, Mukerjee P, Das G, Ahmed R, Chauhan VS. Phenotypic and functional profiling of malaria-
974 induced CD8 and CD4 T cells during blood-stage infection with *Plasmodium yoelii*. Immunology
975 132: 273-286.
976 Chang K-H, Tam M, Stevenson MM. 2004. Modulation of the course and outcome of blood-stage
977 malaria by erythropoietin-induced reticulocytosis. The Journal of Infectious Diseases 189: 735-
978 743.

979 Chau L-Y. 2015. Heme oxygenase-1: emerging target of cancer therapy. Journal of Clinical Science 22:
980 22.
981 Chis Ster I, Niaz HF, Chico ME, Oviedo Y, Vaca M, Cooper PJ. 2021. The epidemiology of soil-transmitted
982 helminth infections in children up to 8 years of age: Findings from an Ecuadorian birth cohort.
983 PLoS Neglected Tropical Diseases 15: e0009972.
984 Choudhury HR, Sheikh NA, Bancroft GJ, Katz DR, de Souza JB. 2000. Early nonspecific immune
985 responses and immunity to blood-stage nonlethal *Plasmodium yoelii* malaria. Infection and
986 Immunity 68: 6127-6132.
987 Clay PA, Rudolf VHW. 2019. How parasite interaction strategies alter virulence evolution in multi-
988 parasite communities. Evolution 73: 2189.
989 Coelho CH, Gazzinelli-Guimaraes PH, Howard J, Barnafo E, Alani NAH, Muratova O, McCormack A,
990 Kelnhofer E, Urban Jr JF, Narum DL, Anderson C, Langhorne J, Nutman TB, Duffy PE. 2019.
991 Chronic helminth infection does not impair immune response to malaria transmission blocking
992 vaccine Pfs230D1-EPA/Alhydrogel® in mice. Vaccine 37: 1038-1045.
993 Comazzetto S, Murphy MM, Berto S, Jeffery E, Zhao Z, Morrison SJ. 2019. Restricted hematopoietic
994 progenitors and erythropoiesis require SCF from leptin receptor+ niche cells in the bone
995 marrow. Cell Stem Cell 24: 477-486.
996 Craig JM, Scott AL. 2017. Antecedent *Nippostrongylus* infection alters the lung immune response to
997 *Plasmodium berghei*. Parasite Immunology 39: e12441.
998 Degarege A, Erko B. 2016. Epidemiology of *Plasmodium* and helminth coinfection and possible reasons
999 for heterogeneity. BioMed Research International 2016: 3083568.
1000 Degarege A, Veledar E, Degarege D, Erko B, Nacher M, Madhivanan P. 2016. *Plasmodium falciparum*
1001 and soil-transmitted helminth co-infections among children in sub-Saharan Africa: a systematic
1002 review and meta-analysis. Parasite Vectors 9: 344.

1003 Dey S, Mazumder S, Siddiqui AA, Iqbal MS, Banerjee C, Sarkar S, De R, Goyal M, Bindu S,
1004 Bandyopadhyay U. 2014. Association of heme oxygenase 1 with the restoration of liver function
1005 after damage in murine malaria by *Plasmodium yoelii*. Infection and Immunity 8: 3113-3126.
1006 De Zuani M, Laznickova P, Tomaskova V, Dvoncovan M, Forte G, Stokin GB, Sramek V, Helan M, Fric J.
1007 2022. High CD4-to-CD8 ratio identifies an at-risk population susceptible to lethal COVID-19.
1008 Scandinavian Journal of Immunology 95: e13125.
1009 Dila KAS, Reda A, Elhady MT, Linh LK, Minh-Duc NT, El-Qushayri AE, Han NL, Mehta V, Hamad WMA,
1010 Eskarous H, Samsom M, Hirayama K, Huy NT. 2022. Association of anthelmintic treatment with
1011 malaria prevalence, incidence, and parasitemia: A systemic review and meta-analysis. Acta
1012 Tropica 225: 106213.
1013 Epiphanio S, Mikolajczak SA, Gonçalves LA, Pamplona A, Portugal S, Albuquerque S, Goldberg M,
1014 Rebelo S, Anderson DG, Akinc A, Vomlocher H-P, Kappe SHI, Soares MP, Mota MM. Heme
1015 oxygenase-1 is an anti-inflammatory host factor that promotes murine *Plasmodium* liver
1016 infection. Cell Host & Microbe 3: 331-338.
1017 Ezenwa VO, Jolles AE. 2011. From host immunity to pathogen invasion: the effects of helminth
1018 coinfection on the dynamics of microparasites. Integrative and Comparative Biology 51: 540.
1019 Fenton A. 2013. Dances with worms: the ecological and evolutionary impacts of deworming on
1020 coinfecting pathogens. Parasitology 140: 1119-1132.
1021 Filbey KJ, Camberis M, Chandler J, Turner R, Kettle AJ, Eichenberger RM, Giacomin P, Le Gros G. 2019.
1022 Intestinal helminth infection promotes IL-5- and $CD4^+$ T cell-dependent immunity in the lung
1023 against migrating parasites. Mucosal Immunology 12: 352-362.
1024 Fortes GB, Alves LS, de Oliveira R, Dutra FF, Rodrigues D, Fernandez PL, Souto-Padron, T, De Rosa MJ,
1025 Kelliher M, Golenbock D, Chan FKM, Bozza MT. 2012. Heme induces programmed necrosis on
1026 macrophages through autocrine TNF and ROS production. Blood 119: 2368-2375.

1027 Frimpong A, Kusi KA, Adu-Gyasi D, Amponsah J, Ofori MF, Ndifon W. 2019. Phenotypic evidence of T
1028 cell exhaustion and senescence during symptomatic *Plasmodium falciparum* malaria. Frontiers
1029 in Immunology 10: 1345.
1030 Graham AL. 2008. Ecological rules governing helminth-microparasite coinfection. PNAS 105: 566.
1031 Gregory RD Montgomery SSJ, Montgomery WI. 1992. Population biology of *Heligmosomoides*
1032 *polygyrus* (Nematoda) in the wood mouse. Journal of Animal Ecology 61: 749-757.
1033 Griffiths EC, Fairlie-Clarke K, Allen JE, Metcalf CJE, Graham AL. 2015. Bottom-up regulation of malaria
1034 population dynamics in mice co-infected with lung-migratory nematodes. Ecology Letters 18:
1035 1387-1396.
1036 Hartgers FC, Yazdanbakhsh M. 2006. Co-infection of helminths and malaria: modulation of the immune
1037 responses to malaria. Parasite Immunology 28: 497.
1038 Helmby H. 2009. Gastrointestinal nematode infection exacerbates malaria-induced liver pathology.
1039 Journal of Immunology 182: 5663.
1040 Howland SW, Claser C, Poh CM, Gun SY, Rénia L. 2015. Pathogenic $CD8^+$ T cells in experimental cerebral
1041 malaria. Seminars in Immunopathology 37: 221-231.
1042 Hürlimann E, Houngbedji CA, Yapi RB, N'Dri PB, Silué KD, Ouattara M, Utzinger J, N'Goran EK, Raso G.
1043 2019. Antagonistic effects of *Plasmodium*-helminth co-infection on malaria pathology in
1044 different population groups in Côte d'Ivoire. PLoS Neglected Tropical Diseases 13: e0007086.
1045 Imai T, Shen J, Chou B, Duan X, Tu L, Tetsutani K, Moriya C, Ishida H, Hamano S, Shimokawa C, Hisaeda
1046 H, Himeno K. 2010. Involvement of $CD8^+$ T cells in protective immunity against murine blood-
1047 stage infection with *Plasmodium yoelii* 17XL strain. European Journal of Immunology 40: 1053-
1048 1061.
1049 Imai T, Ishida H, Suzue K, Taniguchi T, Okada H, Shimokawa C, Hisaeda H. 2015. Cytotoxic activities of
1050 $CD8^+$ T cells collaborate with macrophages to protect against blood-stage murine malaria. eLIFE
1051 4: e04232.

1052 Imrie R, Walsh SK, Roberts KE, Lello J, Longdon B. 2023. Investigating the outcomes of virus coinfection
1053 within and across host species. PLoS Pathogens 19: e1011044.
1054 Immenschuh S, Vijayan V, Janciauskiene S, Gueler F. 2017. Heme as a target for therapeutic
1055 interventions. Frontiers in Pharmacology 8: 146.
1056 Kaiser K, Texier A, Ferrandiz J, Meiller A, Latour C, Peyron F, Cespuglio R, Picot S. 2006. Recombinant
1057 human erythropoietin prevents the death of mice during cerebral malaria. Journal of Infectious
1058 Diseases 193: 987-995.
1059 Karvonen A, Jokela J, Laine A-L. 2019. Importance of sequence and timing in parasite coinfections.
1060 Trends in Parasitology 35: 109-118.
1061 Khan IA, Hakak R, Eberle K, Sayles P, Weiss LM, Urban Jr JF. 2008. Coinfection with *Heligmosomoides*
1062 *polygyrus* fails to establish $CD8^+$ T-cell immunity against *Toxoplasma gondii*. Infection and
1063 Immunity 76: 1305-1313.
1064 Knowles SCL. 2011. The effect of helminth co-infection on malaria in mice: a meta-analysis.
1065 International Journal for Parasitology 41: 1041.
1066 Kolbaum J, Escbach M-L, Steeg C, Jacobs T, Fleischer B, Breloer M. 2012. Efficient control of
1067 *Plasmodium yoelii* infection in BALB/c and C57BL/6 mice with pre-existing *Strongyloides ratti*
1068 infection. Parasite Immunology 34: 388-393.
1069 Kolbaum J, Tartz S, Hartmann W, Helm S, Nagel A, Heussler V, Sebo P, Fleischer B, Jacobs T, Breloer M.
1070 2012. Nematode-induced interference with the anti-Plasmodium $CD8^+$ T-cell response can be
1071 overcome by optimizing antigen administration. European Journal of Immunology 42: 890-900.
1072 Kotepui M, Mala W, Kwankaew P, Kotepui KU, Ramirez Masangkay F, Wilairatana P. 2023. Distinct
1073 cytokine profiles in malaria coinfection: A systematic review. PLoS Neglected Tropical Diseases
1074 17: e0011061.
1075 Kristiansen M, Graversen JH, Jacobsen C, Sonne O, Hoffman HJ, Law SK, Moestrup SK. 2001.
1076 Identification of the haemoglobin scavenger receptor. Nature 409: 198-201.

1077 Kumar S, Bandyopadhyay U. 2005. Free heme toxicity and its detoxification systems in human.
1078 Toxicology Letters 157: 175-188.
1079 Kurup SP, Obeng-Adjei N, Anthony SM, Traore B, Doumbo OK, Butler NS, Crompton PD, Harty JT. 2017.
1080 Regulatory T cells impede acute and long-term immunity to blood-stage malaria through CTLA-
1081 4. Nature Medicine 23: 1220-1227.
1082 Kwan JL, Seitz AE, Fried M, Lee K-L, Metenou S, Morrison R, Kabyemela E, Nutman TB, Prevots DR,
1083 Duffy PE. 2018. Seroepidemiology of helminths and the associations with severe malaria among
1084 infants and young children in Tanzania. PLoS Neglected Tropical Diseases 12: e0006345.
1085 Lin P-H, Chiang M-T, Chau L-Y. 2008. Ubiquitin-proteasome system mediates heme oxygenase-1
1086 degradation through endoplasmatic reticulum-associated degradation pathway. Biochimica et
1087 Biophysica Acta 1783: 1826-1834.
1088 Lippens C, Guivier E, Faivre B, Sorci G. 2016. Reaction norms of host immunity, host fitness and parasite
1089 performance in a mouse - intestinal nematode interaction. International Journal for Parasitology
1090 46: 133-140.
1091 Ma Y, Su X-Z, Lu F. 2020. The roles of Type I interferon in co-infections with parasites and viruses,
1092 bacteria, or other parasites. Frontiers in Immunology 11: 1805.
1093 McBride JA, Striker R. 2017. Imbalance in the game of T cells: What can the CD4/CD8 T-cell ratio tell us
1094 about HIV and health? PLoS Pathogens 13: e1006624.
1095 McLane, L, Abdel-Hakeem MS, Wherry EJ. 2019. CD8 T cell exhaustion during chronic viral infection
1096 and cancer. Annual Review of Immunology 37: 457-495.
1097 Medzhitov R, Schneider DS, Soares MP. 2012. Disease tolerance as a defense strategy. Science 335:
1098 936-941.
1099 Morand S. 1996. Life-history traits in parasitic nematodes: a comparative approach for the search of
1100 invariants. Functional Ecology 10: 210-218.
1101 Nacher M. 2011. Interactions between worms and malaria: good worms or bad worms? Malaria
1102 Journal 10: 259.

1103 Natama HM, Rovira-Vallbona E, Somé MA, Zango SH, Sorgho H, Guetens P, Coulibaly-Traoré M, Valea
1104 I, Mens PF, Schallig HDFH, Kestens L, Tinto H, Rosanas-Urgell A. 2018. Malaria incidence and
1105 prevalence during the first year of life in Nanoro, Burkina Faso: a birth-cohort study. Malaria
1106 Journal 17: 163.
1107 Noland GS, Chowdhury DR, Urban Jr JF, Zavala F, Kumar N. 2010. Helminth infection impairs the
1108 immunogenicity of a *Plasmodium falciparum* DNA vaccine, but not irradiated sporozoites, in
1109 mice. Vaccine 28: 2917-2923.
1110 Noland GS, Graczyk TK, Fried B, Kumar N. 2007. Enhanced malaria parasite transmission from helminth
1111 co-infected mice. American Journal of Tropical Medicine and hygiene 76: 1052.
1112 Noland GS, Urban JF, Fried B, Kumar N. 2008. Counter-regulatory anti-parasite cytokine responses
1113 during concurrent *Plasmodium yoelii* and intestinal helminth infections in mice. Experimental
1114 Parasitology 119: 272-278.
1115 Olatunde AC, Cornwall DH, Roedel M, Lamb TJ. 2022. Mouse models for unravelling immunology of
1116 blood stage malaria. Vaccines 10: 1525.
1117 Paludan SR. 1998. Interleukin-4 and interferon-γ: the quintessence of a mutual antagonistic
1118 relationship. Scandinavian Journal of Immunology 48: 459-468.
1119 Pamplona A, Ferreira A, Balla J, Jeney V, Balla G, Epiphanio S, Chora A, Rodrigues CD, Gregoire IP,
1120 Cunha-Rodrigues M, Portugal S, Soares MP, Mota MM. 2007. Heme oxygenase-1 and carbon
1121 monoxide suppress the pathogenesis of experimental cerebral malaria. Nature Medicine 13:
1122 703–710.
1123 Pascual-Dapena A, Chillaron JJ, Llauradó G, Arnau-Barres I, Flores J, Lopez-Montesinos I, Sorlí L,
1124 Martinez-Pérez JL, Gómez-Zorrilla S, Du J, García-Giralt N, Güerri-Fernández R. 2022. Individuals
1125 with higher CD4/CD8 ratio exhibit increased risk of acute respiratory distress syndrome and in-
1126 hospital mortality during acute SARS-CoV-2 infection. Frontiers in Medicine 9: 924267.

1127 Pelly VS, Kannan Y, Coomes SM, Entwistle LJ, Rückerl D, Seddon B, MacDonald AS, McKenzie A, Wilson
1128 MS. 2016. IL-4-producing ILC2s are required for the differentiation of T_H2 cells following
1129 *Heligmosomoides polygyrus* infection. Mucosal Immunology 9: 1407-1417.
1130 Reynolds LA, Filbey KJ, Maizels RM. 2012. Immunity to the model intestinal helminth parasite
1131 *Heligmosomoides polygyrus*. Seminars in Immunopathology 34: 829-846.
1132 Salazar-Castañón VH, Juárez-Avelar I, Legorreta-Herrera M, Govezensky T, Rodriguez-Sosa M. 2018.
1133 Co-infection: the outcome of *Plasmodium* infection differs according to the time of pre-existing
1134 helminth infection. Parasitology Research 117: 2767.
1135 Salazar-Castañón VH, Legorreta-Herrera M, Rodriguez-Sosa M. 2014. Helminth parasites alter
1136 protection against *Plasmodium* infection. BioMed Research International 2014: 913696.
1137 Scholzen A, Minigo G, Plebanski M. 2009. Heroes or villains? T regulatory cells in malaria infection.
1138 Trends in Parasitology 26: 16-25.
1139 Seixas E, Gozzelino R, Chora A, Ferreira A, Silva G, Larsen R, Rebelo S, Penido C, Smith NR, Coutinho A,
1140 Soares MP. 2009. Heme oxygenase-1 affords protection against noncerebral forms of severe
1141 malaria. Proceedings of the National Academy of Sciences 106: 15837-15842.
1142 Segura M, Matte C, Thawani N, Su Z, Stevenson MM. 2009. Modulation of malaria-induced
1143 immunopathology by concurrent gastrointestinal nematode infection in mice. International
1144 Journal for Parasitology 39: 1525.
1145 Shen S-S, Qu X-Y, Zhang W-Z, Li J, Lv Z-Y. 2019. Infection against infection: parasite antagonism against
1146 parasites, viruses and bacteria. Infectious Diseases of Poverty 8: 49.
1147 Su Z, Segura M, Morgan K, Loredo-Osti JC, Stevenson MM. 2005. Impairment of protective immunity
1148 to blood-stage malaria by concurrent nematode infection. Infection and Immunity 73: 3531-
1149 3539.
1150 Su Z, Segura M, Stevenson MM. 2006. Reduced protective efficacy of a blood-stage malaria vaccine by
1151 concurrent nematode infection. Infection and Immunity 74: 2138-2144.

1152 Supali T, Verweij JJ, Wiria AE, Djuardi Y, Hamid F, Kaisar MMM, Wammes LJ, van Lieshout L, Luty AJF,
1153 Sartoro E, Yazdanbakhsh M. 2010. Polyparasitism and its impact on the immune system.
1154 International Journal for Parasitology 40: 1171-1176.
1155 Suzuki N, Ohneda O, Takahashi S, Higuchi M, Mukai HY, Nakahata T, Imagawa S, Yamamoto M. 2002.
1156 Erythroid-specific expression of the erythropoietin receptor rescued its null mutant mice from
1157 lethality. Blood 100: 2279-2288.
1158 Szabo E, Bowhay C, Forrester E, Liu H, Dong B, Coria AL, Perera S, Fung B, Badawadagi N, Gaio C, Bailey
1159 K, Ritz M, Bowron J, Ariyaratne A, Finney CAM. 2024. *Heligmosomoides bakeri* and *Toxoplasma*
1160 *gondii* co-infection leads to increased mortality associated with changes in immune resistance
1161 in the lymphoid compartment and disease pathology. PLoS ONE 19: e02922408.
1162 Tadesse FG, van den Hoogen L, Lanke K, Schildkraut J, Tetteh K, Aseffa A, Mamo H, Sauerwein R, Felger
1163 I, Drakeley C, Gadissa E, Bousema T. 2017. The shape of the iceberg: quantification of
1164 submicroscopic *Plasmodium falciparum* and *Plasmodium vivax* parasitemia and gametocytemia
1165 in five low endemic settings in Ethiopia. Malaria Journal 16: 99.
1166 Tetsutani K, Ishiwata K, Ishida H, Tu L, Torii M, Hamano S, Himeno K, Hisaeda H. 2009. Concurrent
1167 infection with *Heligmosomoides polygyrus* suppresses anti-*Plasmodium yoelii* protection
1168 partially by induction of $CD4^{+}CD25^{+}Foxp3^{+}$ Treg in mice. European Journal of Immunology 39:
1169 2822-2830.
1170 Trape J-F, Diagne N, Diene-Sarr F, Faye J, Dieye-Ba F, Bassène H, Badiane A, Bouganali C, Tall A, Ndiaye
1171 R, Doucouré S, Wotodjo AN, Vigan-Womas I, Guillotte-Blisnick M, Talla C, Niang M, Touré-Baldé
1172 A, Perraut R, Roussilhon C, Druilhe P, Rogier C, Mercereau-Puijalon O, Loucoubar C, Sokhnab C.
1173 2024. One hundred malaria attacks since birth. A longitudinal study of African children and
1174 young adults exposed to high malaria transmission. eClinicalMedicine 67: 102379.
1175 Tsubata S, Ebe K, Kawamura T, Ishimoto Y, Tomiyama-Miyaji C, Watanabe H, Sekikawa H, Aoyagi Y,
1176 Abo T. 2005. Protection against malaria by anti-erythropoietin antibody due to suppression of
1177 erythropoiesis in the liver and at other sites. Immunology and Cell Biology 83: 638-642.

1178 Viney ME, Graham AL. 2013. Patterns and processes in parasite co-infection. Advances in Parasitology
1179 82: 321-369.
1180 Wait LF, Kamiya T, Fairlie-Clarke KJ, Metcalf CJE, Graham AL, Mideo N. 2021. Differential drivers of
1181 intraspecific and interspecific competition during malaria-helminth co-infection. Parasitology
1182 148: 1030-1039.
1183 Webb EL, Ekii AO, Pala P. 2012. Epidemiology and immunology of helminth-HIV interactions. Current
1184 Opinion in HIV and AIDS 7: 245-253.
1185 Wykes MN, Lewin SR. 2018. Immune checkpoint blockade in infectious diseases. Nature Reviews
1186 Immunology 18: 91-104.
1187 Xing Z, Liu S, He X. 2024. Critical and diverse role of alarmin cytokines in parasitic infections. Frontiers
1188 in Cellular and Infection Microbiology 14: 1418500.